*Chem. Sci.*

# Efficient stabilisation of a dihydrogenphosphate tetramer and a dihydrogenpyrophosphate dimer by a cyclic pseudopeptide containing 1,4-disubstituted 1,2,3-triazole moieties

Disha Mungalpara,[a] Arto Valkonen,[b] Kari Rissanen,[b] and Stefan Kubik*[,a]

[a] *Technische Universität Kaiserslautern, Fachbereich Chemie - Organische Chemie, Erwin-Schrödinger-Straße, 67663 Kaiserslautern, Germany, Fax: +49-631-205-3921, Email: kubik@chemie.uni-kl.de*

[b] *University of Jyväskylä, Department of Chemistry, Nanoscience Center, P.O. Box 35, Jyväskylä FI-40014, Finland.*

.

## CONTENT

Synthetic Procedures

**General details**. Analyses were carried out as follows: melting points, Müller SPM-X 300; NMR, Bruker DPX 400 (peak assignments were confirmed by using H,H-COSY and HMQC spectra, spectra were referenced to the residual solvent signals (DMSO-$d_6$: $\delta_H$ = 2.50 ppm, $\delta_C$ = 39.5 ppm);[1] MALDI-TOF-MS, BrukerUltraflex TOF/TOF; elemental analysis, Elementar vario Micro cube; optical rotation, Perkin Elmer 241 MC digital polarimeter ($d$ = 10 cm); ITC, Microcal VP-ITC.

The following abbreviations are used: TBA, tetrabutylammonium; Epa, 2-amino-6-ethynyl-2-pyridine; Lac, $CH_3CHCO$; Tri, 1,2,3-triazole; PyCloP, chlorotripyrrolidinophosphonium hexafluoro-phosphate; TBTA, tris[(1-benzyl-1*H*-1,2,3-triazol-4-yl)methyl]amin; TBAF, tetrabutylammonium fluoride; DHP, dihydrogenphosphate; HPP, hydrogenpyrophosphate, DHPP, dihydrogenpyro-phosphate.

The synthesis of the linear pseudopeptide **4** is described elsewhere.[2] TBA sulfate, TBA DHP, TBA HPP, and TBA DHPP are commercially available and were used after confirming purity by elemental analysis.

**ESI MS measurements**. These measurements were performed by using a Paul-type quadrupole ion trap instrument (AmaZonETD, Bruker Daltonics). The ion source was set to negative electrospray ionisation mode. Scan speed was 32500 ($m/z$) $s^{-1}$ in standard resolution scan mode (0.3 FWHM / $m/z$). Mass spectra were accumulated for at least two minutes. Sample solutions were continuously infused into the ESI chamber by a syringe pump at a flow rate of 2 μL $min^{-1}$. Nitrogen was used as drying gas with a flow rate of 3.0 L $min^{-1}$ at 220 °C. The solutions were sprayed at a nebulizer pressure of 280 mbar (4 psi) and the electrospray needle was held at 4.5 kV.

**H-Epa-(*R*)-Lac-1,4-Tri-Epa-(*S*)-Lac-OMs**.

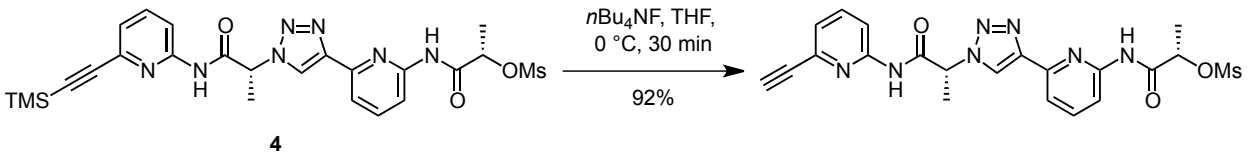


**4**

Compound **4** (3.3 g, 5.9 mmol) was dissolved in THF (40 mL) at 0 °C. To this solution, a solution of TBAF trihydrate (3.7 g, 11.8 mmol) in THF (20 mL) was added dropwise. This mixture was stirred

for 30 min at 0 °C. Ethyl acetate (50 mL) and water (50 mL) were added, and after separation of the organic layer the aqueous phase was extracted three times using ethyl acetate (150 mL). The combined organic layers were dried using $MgSO_4$. The solvent was evaporated and the residue purified on silica gel column with hexane/ethyl acetate, 1:1 (*v/v*) as eluent. The product was obtained as a white powder. Yield: 2.6 g (5.4 mmol, 92%); MS (MALDI-TOF) *m/z* (%): $[M–CH_3SO_3H+H]^+$ 388.2 (100), $[M+H]^+$ 484.3 (35), $[M+Na]^+$ 506.3 (48), $[M+K]^+$ 522.3 (8).

**TMS-Epa-(R)-Lac-1,4-Tri-Epa-(R)-Lac-$N_3$.**

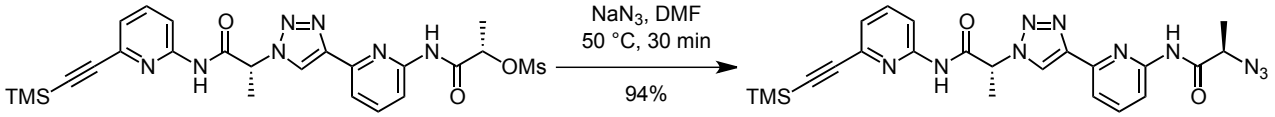


**4**

Compound **4** (3.3 g, 5.9 mmol) and sodium azide (600 mg, 9.2 mmol) were dissolved in DMF (20 mL). The mixture was stirred at 50 °C for 30 min. After adding ethyl acetate (100 mL) and water (100 mL) the aqueous layer was extracted with ethyl acetate (3 × 100 mL). The combined organic layers were dried using $MgSO_4$. Pure product was obtained by column chromatography with hexane/ethyl acetate, 1:1 (*v/v*) as the eluent. Yield: 2.8 g (5.6 mmol, 94%); MS (MALDI-TOF) *m/z* (%): $[M–N_2+H_2+H]^+$ 477.3 (14), $[M+H]^+$ 503.3 (100), $[M+Na]^+$ 525.3 (25).

**TMS-Epa-[(*R*)-Lac-1,4-Tri-Epa]$_3$-(*S*)-Lac-OMs (5).**

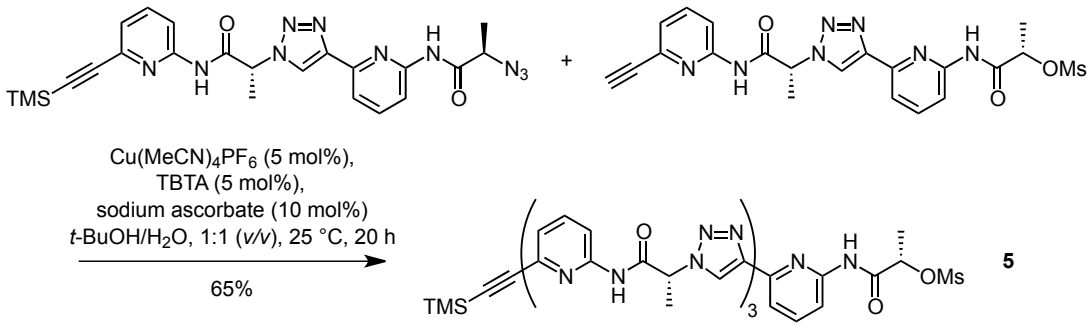


**5**

H-Epa-(*R*)-Lac-1,4-Tri-Epa-(*S*)-Lac-OMs (2.6 g, 5.4 mmol) and TMS-Epa-(*R*)-Lac-1,4-Tri-Epa-(*R*)-Lac-$N_3$ (2.8 g, 5.6 mmol) were dissolved in *t*-BuOH/$H_2O$, 1:1 (*v/v*) (300 mL), followed by the addition of a solution of TBTA (143 mg, 270 µmol, 5 mol%), $Cu(MeCN)_4PF_6$ (101 mg, 270 µmol, 5 mol%), and sodium ascorbate (107 mg, 540 µmol, 10 mol%) in *t*-BuOH/$H_2O$, 1:1 (*v/v*) (20 mL). The reaction mixture was stirred at 25 °C for 20 h and extracted with ethyl acetate three times (3 × 20 mL). The

combined organic layers were washed with water twice and dried over $MgSO_4$. The solvent was evaporated and the residue was purified by column chromatography using ethyl acetate as the eluent. Pure product was obtained as a white solid. NMR indicated that the product thus obtained contained traces of ethyl acetate, which is why it was not characterised by elemental analysis. Purity was high enough for the next step. Yield: 3.5 g (3.5 mmol, 65%); m.p. > 200 °C (dec); $^1$H NMR (400 MHz, 25 °C, DMSO-$d_6$) δ = 11.44 (s, 1H, NH), 11.25 (s, 2H, NH), 10.79 (s, 1H, NH), 8.66 (s, 1H, TriH), 8.65 (s, 1H, TriH), 8.64 (s, 1H, TriH), 7.91-8.05 (m, 7H, EpaH(4)+EpaH(3)), 7.84 (t, 1H, $^3J$(H, H) = 8.0 Hz, EpaH(4)), 7.79 (d, 3H, $^3J$(H, H) = 7.6 Hz, EpaH(5)), 7.32 (dd, 1H, $^3J$(H, H) = 7.5 Hz, $^4J$(H, H) = 0.7 Hz, EpaH(5)), 5.88 (m, 2H, LacCH), 5.77 (q, 1H, $^3J$(H, H) = 7.1 Hz, LacCH), 5.34 (q, 1H, $^3J$(H, H) = 6.4 Hz, LacCH), 3.27 (s, 3H, $MsCH_3$), 1.85-1.89 (m, 9H, $LacCH_3$), 1.55 (d, 3H, $^3J$(H, H) = 6.7 Hz, $LacCH_3$), 0.25 (s, 9H, $TMSCH_3$) ppm; $^{13}$C NMR (100.6 MHz, DMSO-$d_6$) δ = 168.2 (CO), 168.1 (CO), 151.5 (EpaC(2)), 151.2 (EpaC(2)), 151.1 (EpaC(2)), 148.5 (EpaC(6)), 148.6 (EpaC(6)), 146.5 (TriC(4)), 146.4 (TriC(4)), 140.1 (EpaC(6)), 139.7 (EpaC(4)), 139.6 (EpaC(4)), 139.4 (EpaC(4)), 123.2 (EpaC(5)), 122.9 (TriC(5)), 122.8 (TriC(5)), 116.0 (EpaC(5)), 115.9 (EpaC(5)), 114.0 (EpaC(3)) 113.0 (EpaC(3)), 112.9 (EpaC(3)), 103.4 (Si–C≡C), 94.2 (Si–C≡C), 75.3 (LacC), 58.8 (LacC), 58.7 (LacC), 38.1 ($MsCH_3$), 18.7 ($LacCH_3$), 18.1 ($LacCH_3$), 18.0 ($LacCH_3$), 17.9 ($LacCH_3$), –0.4 ($TMSCH_3$) ppm; MS (MALDI-TOF) *m/z* (%): $[M–Si(CH_3)_3+2H]^+$ 914.4 (37), $[M–CH_3SO_3+H+K]^+$ 930.4 (13), $[M+Na]^+$ 1008.4 (100), $[M+K]^+$ 1024.4 (19).

**H-Epa-[(*R*)-Lac-1,4-Tri-Epa]$_3$-(*S*)-Lac-OMs**.

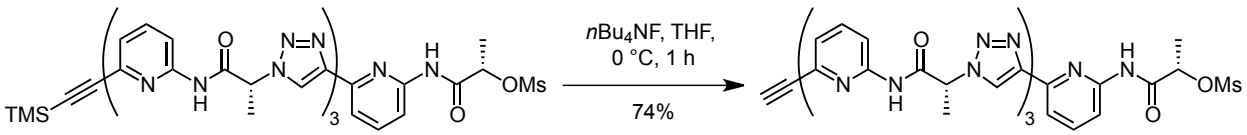


**5**

Compound **5** (3.4 g, 3.5 mmol) was dissolved in THF (40 mL) at 0 °C. To this solution, a solution of TBAF trihydrate (2.2 g, 7.0 mmol) in THF (20 mL) was added dropwise. The reaction mixture was stirred for 1 h at 0 °C. Ethyl acetate (150 mL) and water (150 mL) were added, and the organic layer was separated. The aqueous layer was extracted four times with ethyl acetate (4 × 50 mL), and the combined organic layers were dried using $MgSO_4$. The solvent was evaporated, and the residue purified on a silica gel column with ethyl acetate as eluent. The product was obtained as a white

powder. Yield: 2.4 g (2.6 mmol, 74%); MS (MALDI-TOF) *m/z* (%): $[M–CH_3SO_3H+H]^+$ 818.4 (93), $[M+H]^+$ 914.4 (100), $[M+Na]^+$ 936.4 (15).

**H-Epa-[(*R*)-Lac-1,4-Tri-Epa]$_3$-(*R*)-Lac-N$_3$.**

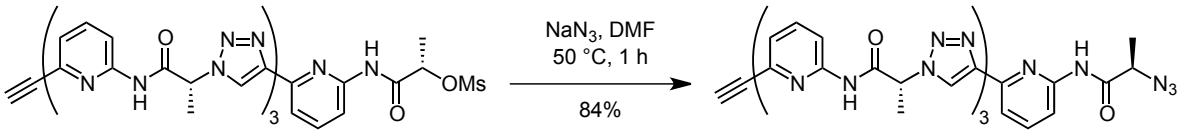


This reaction was performed with 0.19 mmol of starting material to avoid having to store larger amounts of the product, which is potentially prone to oligomerisation via thermal 1,3-dipolar cycloaddition, and because the subsequent cyclisation step turned out to be more efficient when performed on a smaller scale. H-Epa-[(*R*)-Lac-1,4-Tri-Epa]$_3$-(*S*)-Lac-OMs (170 mg, 0.19 mmol) and sodium azide (250 mg, 0.36 mmol) were dissolved in DMF (10 mL), and the reaction mixture was heated at 50 °C for 1 h. Ethyl acetate (30 mL) and water (30 mL) were added, and the organic layer was separated. The aqueous layer was extracted three times with ethyl acetate (3 × 50 mL), and the combined organic layers were dried over $MgSO_4$. The solvent was evaporated and the residue purified on a silica gel column with ethyl acetate as the eluent to afford pure product as a white powder. Yield: 135 mg (0.16 mmol, 84%); MS (MALDI-TOF) *m/z* (%): $[M–N_2+H_2+H]^+$ 835.6 (14), $[M+H]^+$ 861.6 (100), $[M+Na]^+$ 883.6 (86).

***cyclo*[(*R*)-Lac-1,4-Tri-Epa]$_4$ (2).**

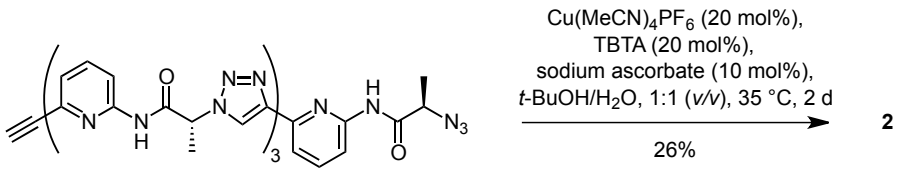


H-Epa-[(*R*)-Lac-1,4-Tri-Epa]$_3$-(*R*)-Lac-N$_3$ (130 mg, 151 µmol) was dissolved in a mixture of DMF (20 mL) and *t*-BuOH/$H_2O$, 1:1 (*v/v*) (50 mL). The resulting solution was added to a suspension of TBTA (8 mg, 15 µmol, 10 mol%), sodium ascorbate (3.0 mg, 15 µmol, 10 mol%), and $Cu(MeCN)_4PF_6$ (6 mg, 16 µmol, 10 mol%) in *t*-BuOH/$H_2O$, 1:1 (*v/v*) (250 mL). The reaction mixture was stirred at 35 °C and progress was followed by HPLC. Additional solid TBTA (9 mg, 18 µmol, 10 mol %) and $Cu(MeCN)_4PF_6$ (7 mg, 18 µmol, 10 mol%) were added every 24 h until HPLC

indicated full conversion, typically after 2 d. Ethyl acetate was added to the reaction mixture and the aqueous layer was removed. The organic solvent was evaporated, and the residue was purified on flash silica gel column using a gradient of dichloromethane/acetone (5:1, 3:2, 1:1, 1:2, pure acetone) to afford ca. 95 % pure product. Pure product was obtained after another chromatographic step using the same solvent mixtures as eluents. Yield: 34 mg (40 μmol, 26%); m.p. > 200 °C (dec); $[\alpha]_D^{25}$ = –31.0 (*c* = 0.1, DMSO); $^1$H NMR (400 MHz, 25 °C, DMSO-$d_6$) δ = 10.80 (s, 4H, NH), 8.67 (s, 4H, TriH), 7.96 (d, 4H, $^3J$(H, H) = 7.3 Hz, EpaH(4)), 7.89 (t, 4H, $^3J$(H, H) = 7.8 Hz, EpaH(5)), 7.76 (d, 4H, $^3J$(H, H) = 8.0 Hz, EpaH(3)), 5.66-5.78 (m, 4H, LacCH), 1.85 (d, 9H, $^3J$(H, H) = 7.1 Hz, $LacCH_3$); $^{13}$C NMR (100.6 MHz, 25 °C, DMSO-$d_6$) δ = 167.4 (CO), 151.2 (EpaC(2)), 148.4 (EpaC(6)), 146.1 (TriC(4)), 139.5 (EpaC(4)), 123.9 (TriC(5)), 115.8 (EpaC(5)), 112.9 (EpaC(3)), 59.0 (LacC), 17.2 ($LacCH_3$); MS (MALDI-TOF) *m/z* (%): $[M+Na]^+$ 883.3 (100), $[M+K]^+$ 899.4 (29); elemental analysis calcd (%) for $C_{40}H_{36}N_{20}O_4 \cdot 6.5H_2O$: C 49.13, N 28.65, H 5.05 found C 49.20, N 28.58, H 5.48.

MALDI-TOF MS: H-Epa-(*R*)-Lac-1,4-Tri-Epa-(*S*)-Lac-OMs (positive mode).

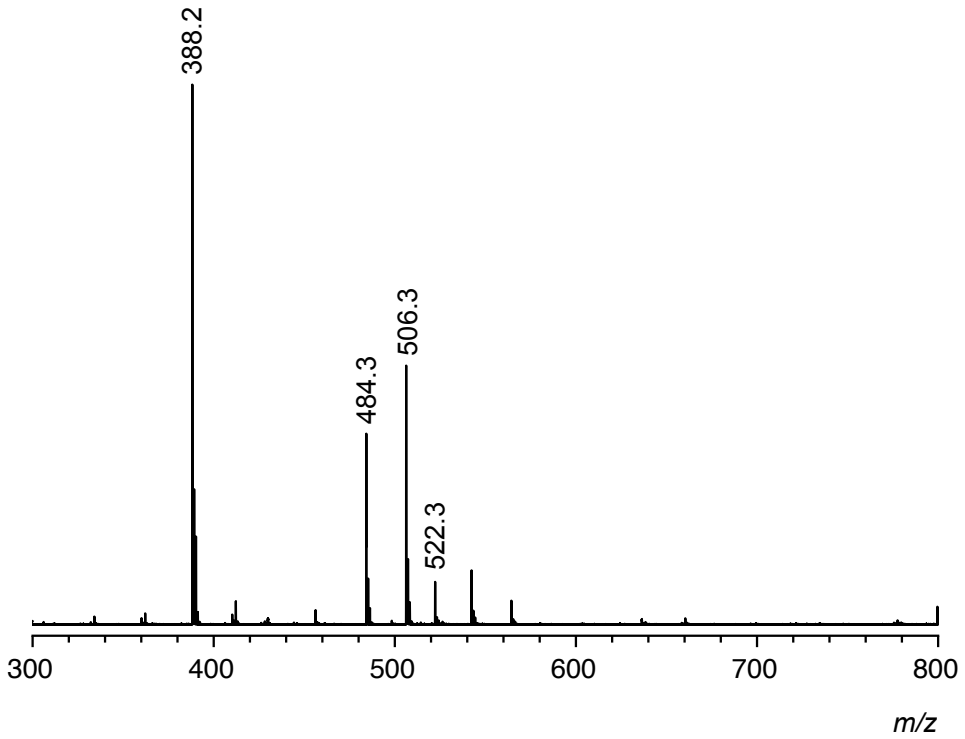


| | | *m/z calcd.* | *m/z exp.* |
|---|---|---|---|
| $[M–CH_3SO_3H+H]^+$ | $C_{21}H_{21}N_7O_5S – CH_3SO_3H + H^+$ | 388.2 | 388.2 |
| $[M+H]^+$ | $C_{21}H_{21}N_7O_5S + H^+$ | 484.1 | 484.3 |
| $[M+Na]^+$ | $C_{21}H_{21}N_7O_5S + Na^+$ | 506.1 | 506.3 |
| $[M+K]^+$ | $C_{14}H_{20}N_2O_4SSi + Na^+$ | 522.1 | 522.3 |

MALDI-TOF MS: TMS-Epa-(*R*)-Lac-1,4-Tri-Epa-(*R*)-Lac-$N_3$ (positive mode).

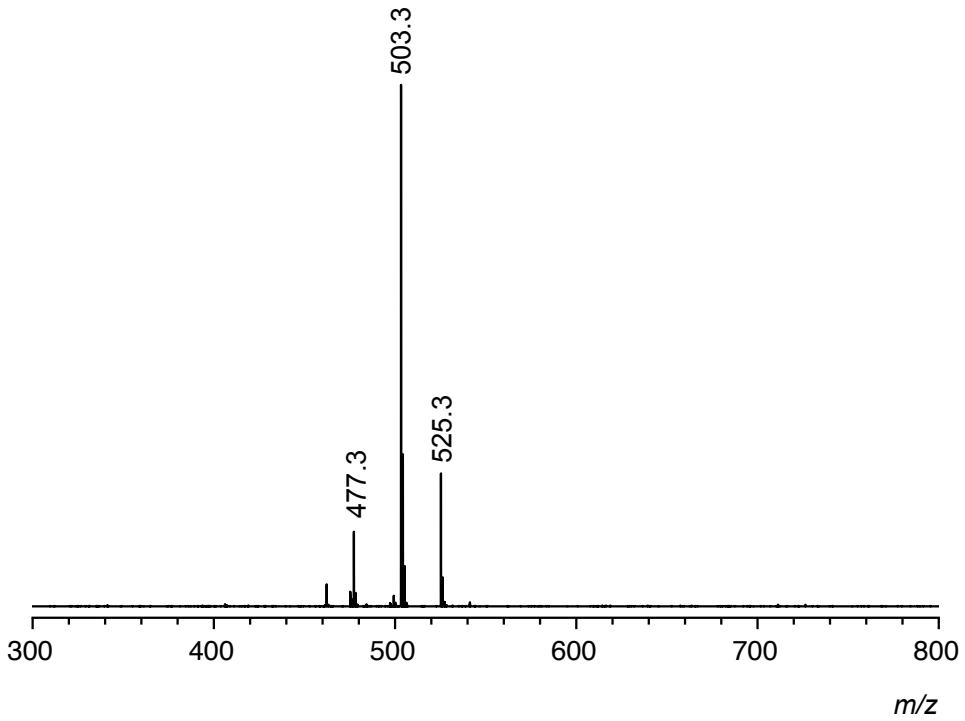


| | | *m/z calcd.* | *m/z exp.* |
|---|---|---|---|
| $[M–N_2+H_2+H]^+$ | $C_{23}H_{28}N_8O_2Si + H^+$ | 477.2 | 477.3 |
| $[M+H]^+$ | $C_{23}H_{26}N_{10}O_2Si + H^+$ | 503.2 | 503.3 |
| $[M+Na]^+$ | $C_{23}H_{26}N_{10}O_2Si + Na^+$ | 525.2 | 525.3 |

$^{1}$H NMR: TMS-Epa-[(*R*)-Lac-1,4-Tri-Epa]$_3$-(*S*)-Lac-OMs **5** (400 MHz, DMSO-$d_6$, 25 °C).

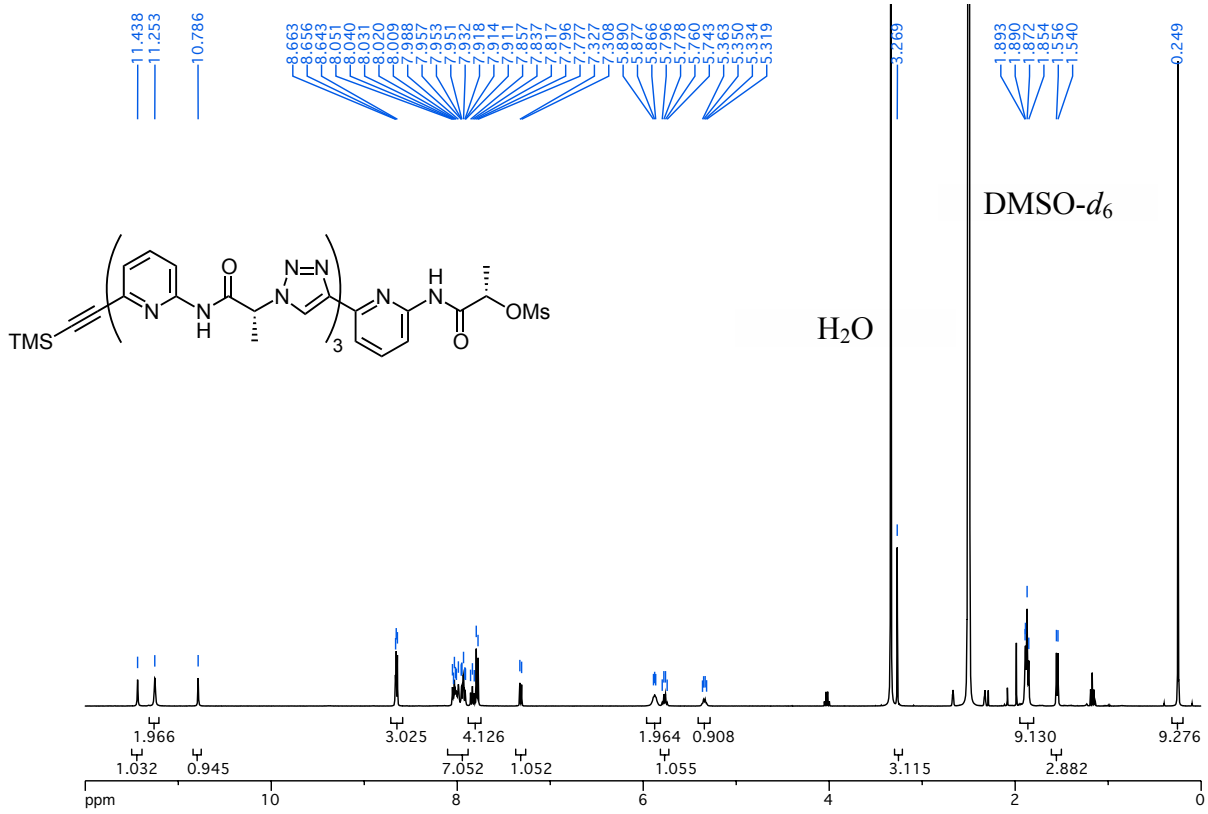


$^{13}$C NMR: TMS-Epa-[(*R*)-Lac-1,4-Tri-Epa]$_3$-(*S*)-Lac-OMs **5** (100.6 MHz, DMSO-$d_6$, 25 °C).

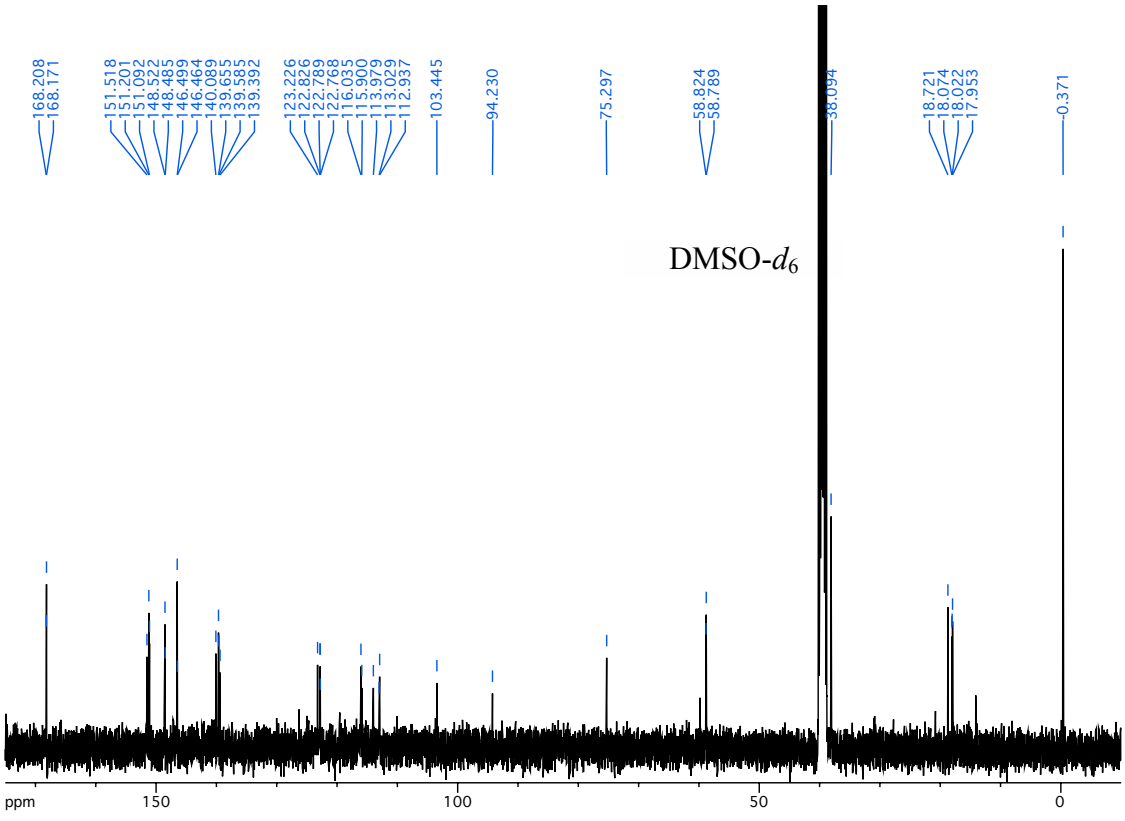

MALDI-TOF MS: TMS-Epa-[(*R*)-Lac-1,4-Tri-Epa]$_3$-(*S*)-Lac-OMs **5** (positive mode).

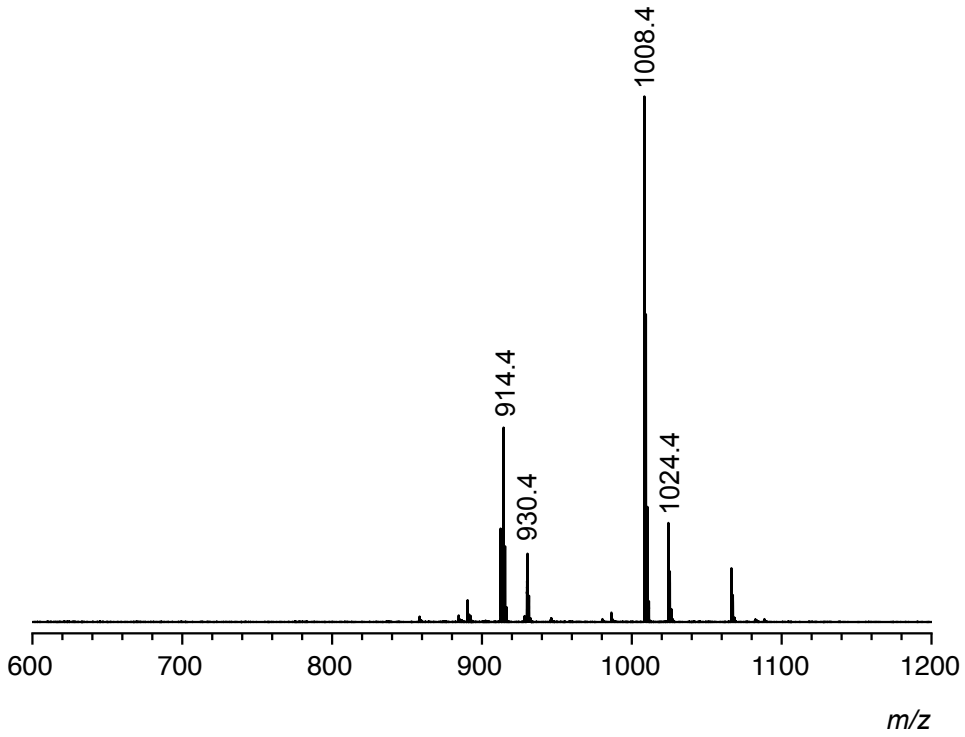


| | | *m/z calcd.* | *m/z exp.* |
|---|---|---|---|
| $[M–Si(CH_3)_3+2H]^+$ | $C_{41}H_{39}N_{17}O_7S + H^+$ | 914.3 | 914.4 |
| $[M–CH_3SO_3+H+K]^+$ | $C_{43}H_{45}N_{17}O_4Si + Na^+$ | 930.3 | 930.4 |
| $[M+Na]^+$ | $C_{44}H_{47}N_{17}O_7SSi + Na^+$ | 1008.3 | 1008.4 |
| $[M+K]^+$ | $C_{44}H_{47}N_{17}O_7SSi + K^+$ | 1024.3 | 1024.4 |

MALDI-TOF MS: H-Epa-[(*R*)-Lac-1,4-Tri-Epa]$_3$-(*S*)-Lac-OMs (positive mode).

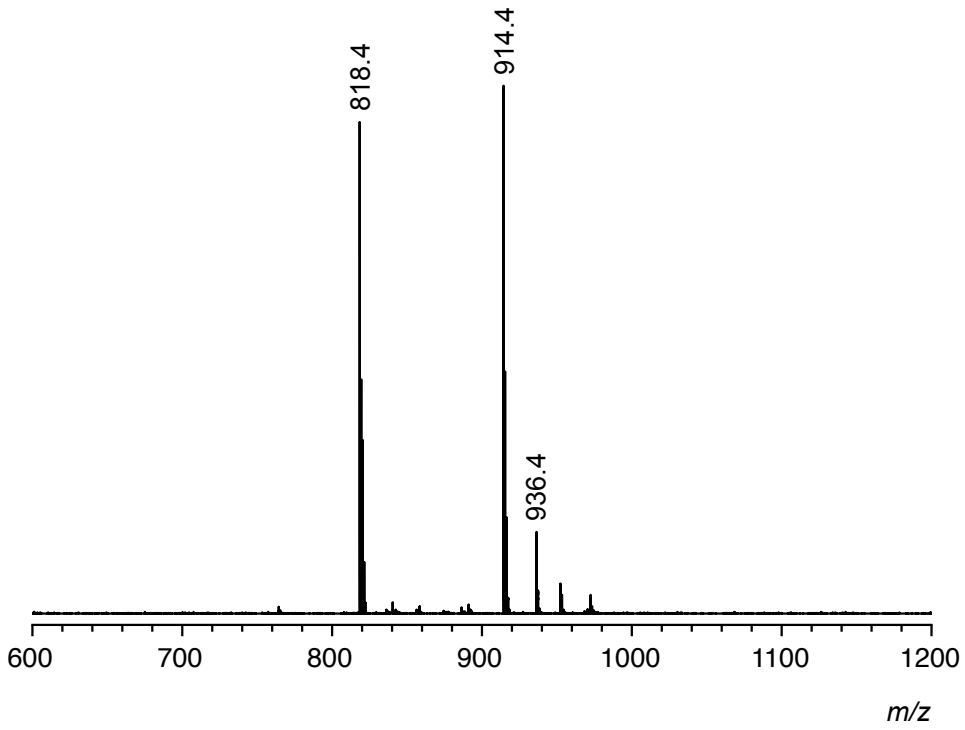


| | | *m/z calcd.* | *m/z exp.* |
|---|---|---|---|
| $[M–CH_3SO_3H+H]^+$ | $C_{40}H_{35}N_{17}O_4 + H^+$ | 818.3 | 818.4 |
| $[M+H]^+$ | $C_{41}H_{39}N_{17}O_7S + H^+$ | 914.3 | 914.4 |
| $[M+Na]^+$ | $C_{41}H_{39}N_{17}O_7S + Na^+$ | 936.3 | 936.4 |

MALDI-TOF MS: H-Epa-[(*R*)-Lac-1,4-Tri-Epa]$_3$-(*R*)-Lac-$N_3$ (positive mode).

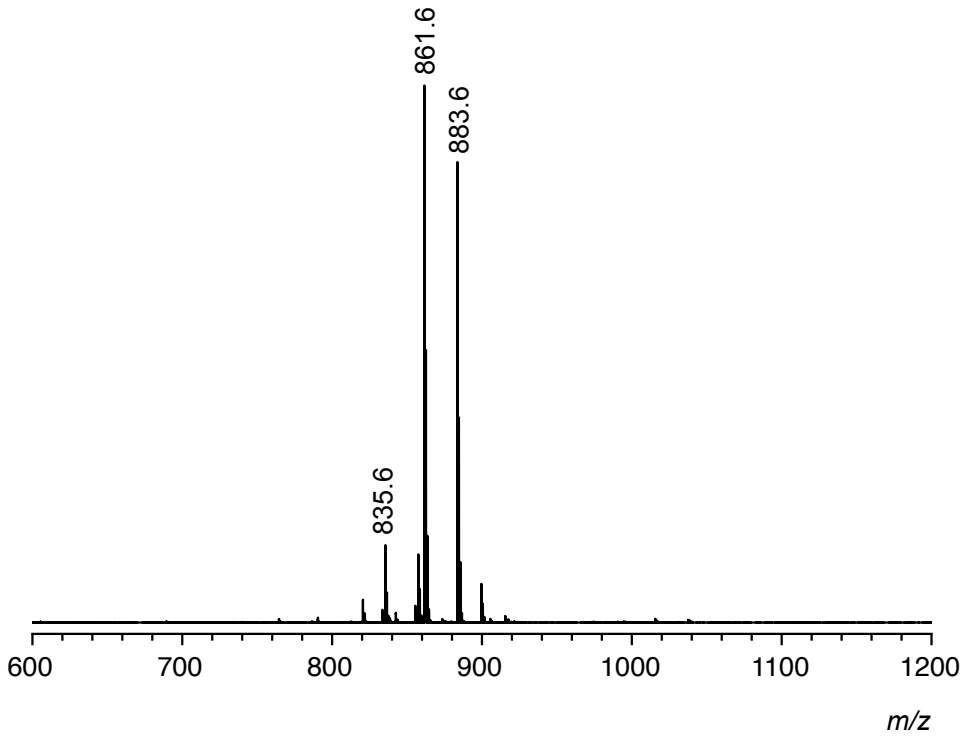


| | | *m/z calcd.* | *m/z exp.* |
|---|---|---|---|
| $[M–N_2+H_2+H]^+$ | $C_{40}H_{38}N_{18}O_4 + H^+$ | 835.3 | 835.6 |
| $[M+H]^+$ | $C_{40}H_{36}N_{20}O_4 + H^+$ | 861.3 | 861.6 |
| $[M+Na]^+$ | $C_{40}H_{36}N_{20}O_4 + Na^+$ | 883.3 | 883.6 |

$^{1}$H NMR: **2** (400 MHz, DMSO-$d_6$, 25 °C).

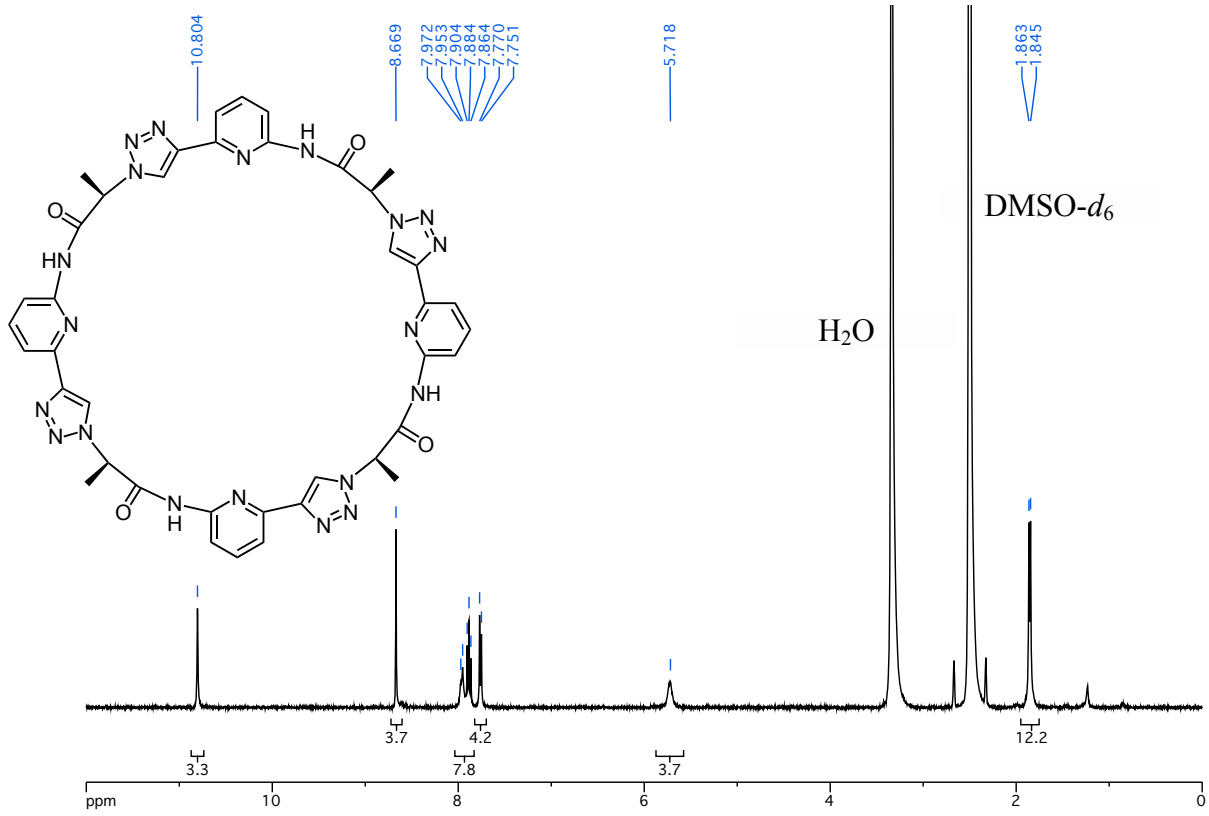


$^{13}$C NMR: **2** (100.6 MHz, DMSO-$d_6$, 25 °C).

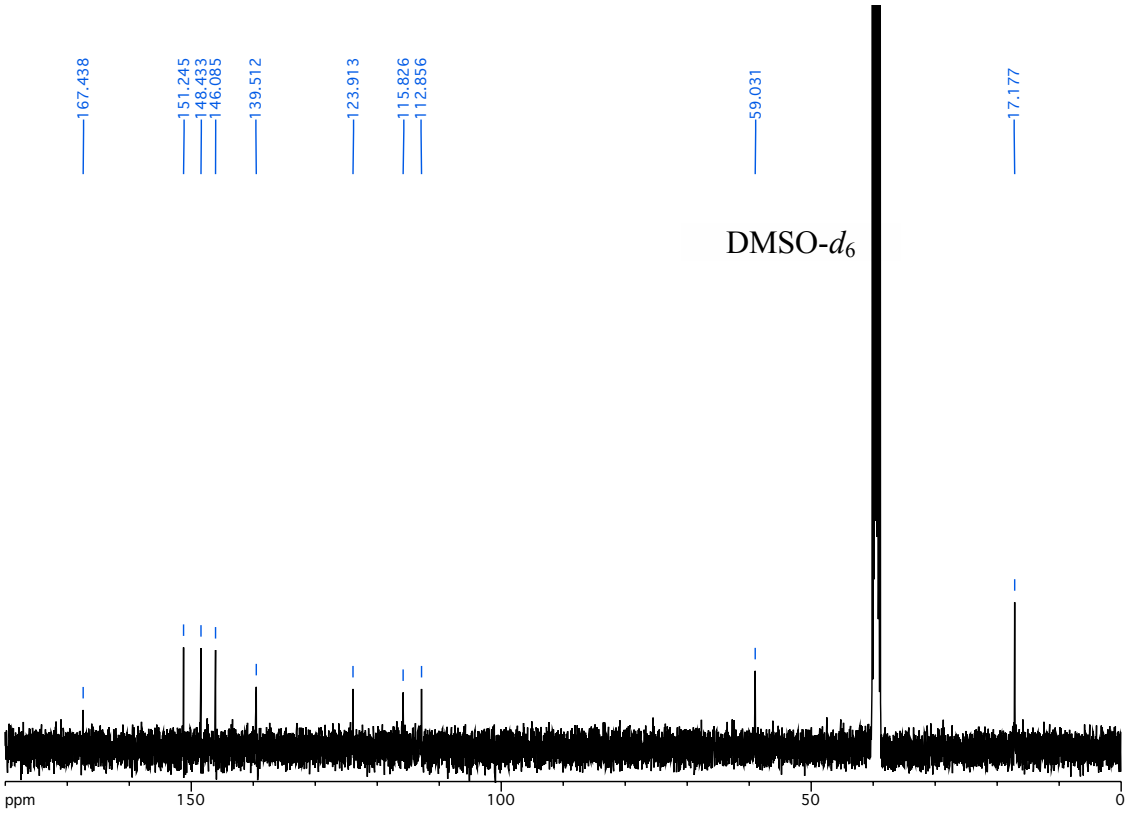

MALDI-TOF MS: **2** (positive mode).

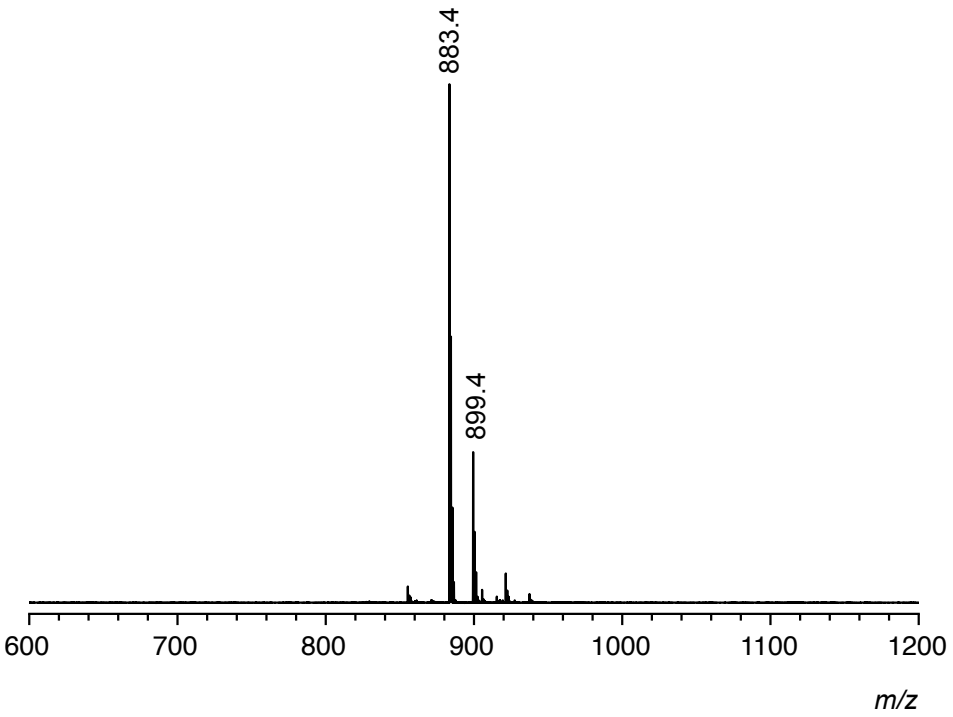


| | | *m/z calcd.* | *m/z exp.* |
|---|---|---|---|
| $[M+Na]^+$ | $C_{40}H_{36}N_{20}O_4 + Na^+$ | 883.3 | 883.4 |
| $[M+K]^+$ | $C_{40}H_{36}N_{20}O_4 + K^+$ | 899.3 | 899.4 |

NOESY NMR Spectrum: **2** (1 mM) in DMSO-$d_6$ (mixing time 300 ms) (400 MHz, 25 °C).

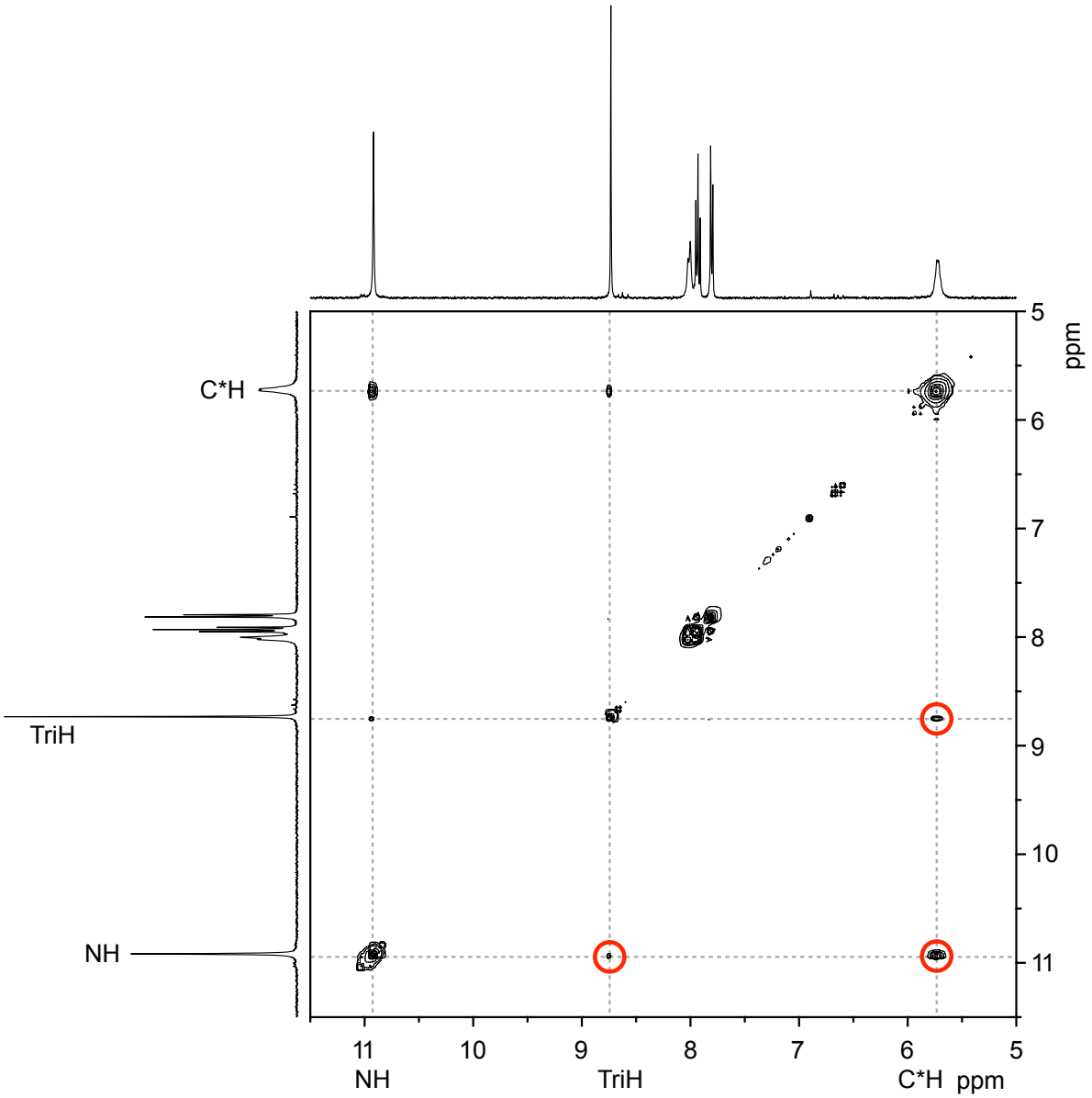

ROESY NMR Spectrum: **2** (0.5 mM) in DMSO-$d_6$ (mixing time 300 ms) in the presence of 1 equiv of tetrabutylammonium dihydrogenpyrophosphate (400 MHz, 25 °C, red - positive, blue - negative).

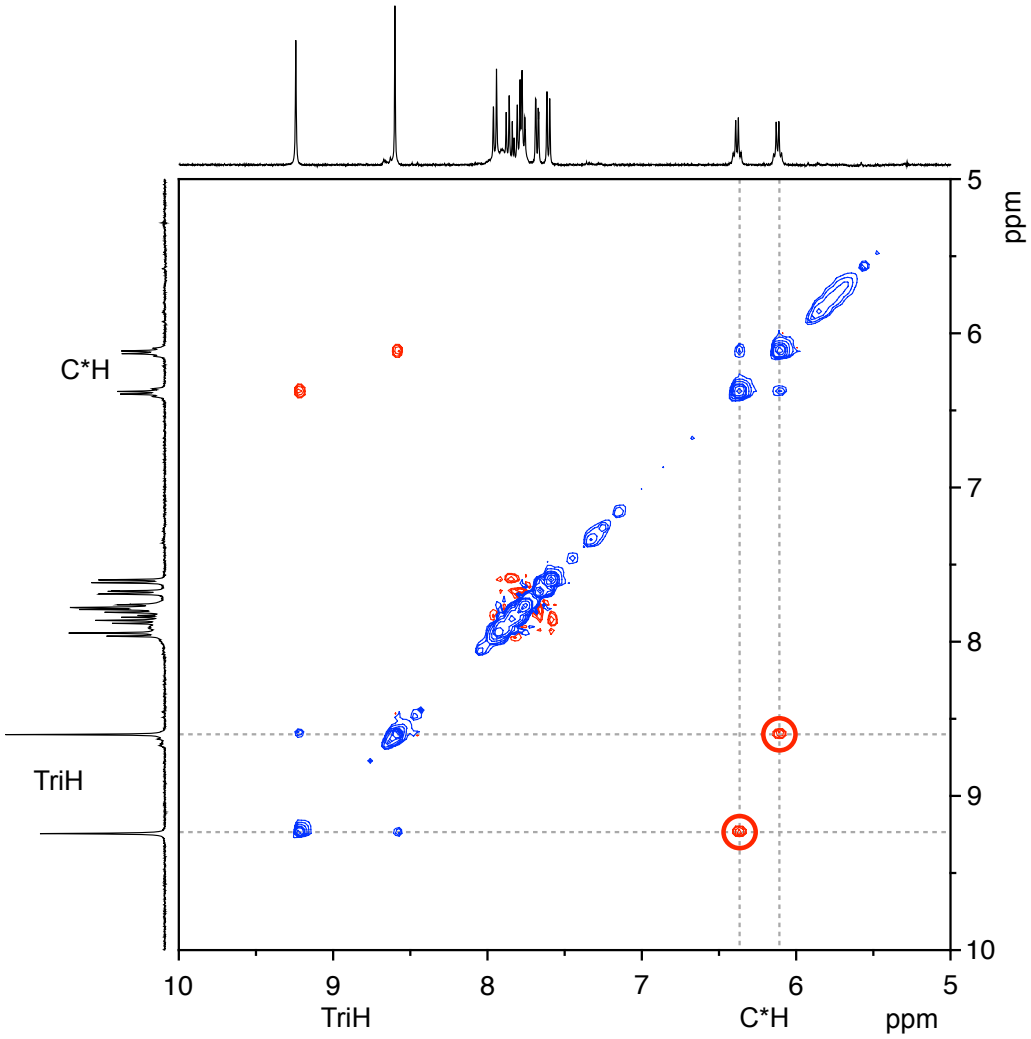

$^{1}$H NMR Spectra: **1** (0.5 mM) in 2.5 vol% $D_2O$/DMSO-$d_6$ in the absence (a) and the presence of 0.50 equiv (b), 1.00 equiv (c), and 2.00 equiv (d) of TBA sulfate. The signals of the triazole and C*H protons are marked in green and blue, respectively.

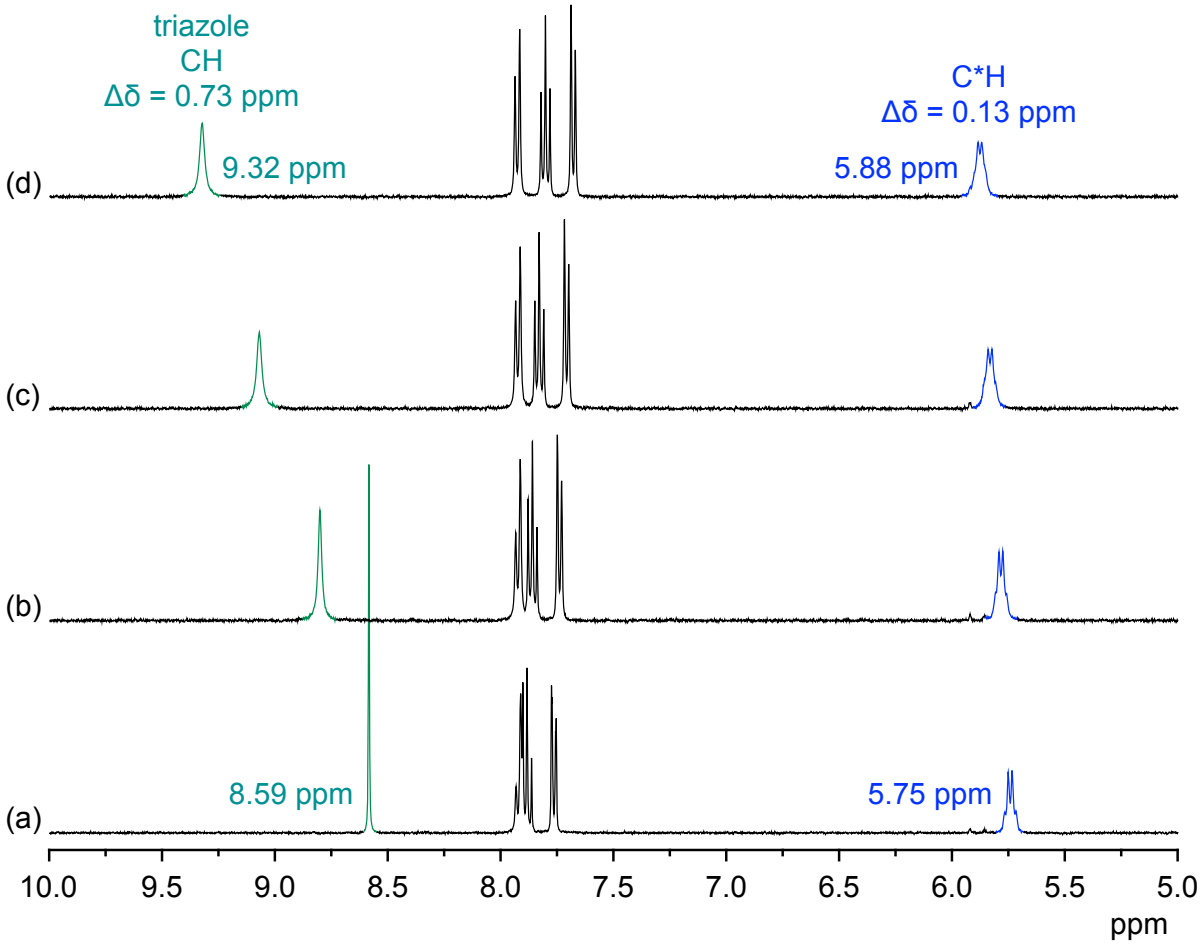

$^{1}$H NMR Spectra: **2** (0.5 mM) in 2.5 vol% $D_2O$/DMSO-$d_6$ in the absence (a) and the presence of 0.50 equiv (b), 1.00 equiv (c), and 2.00 equiv (d) of TBA sulfate. The signals of the triazole and C*H protons are marked in green and blue, respectively.

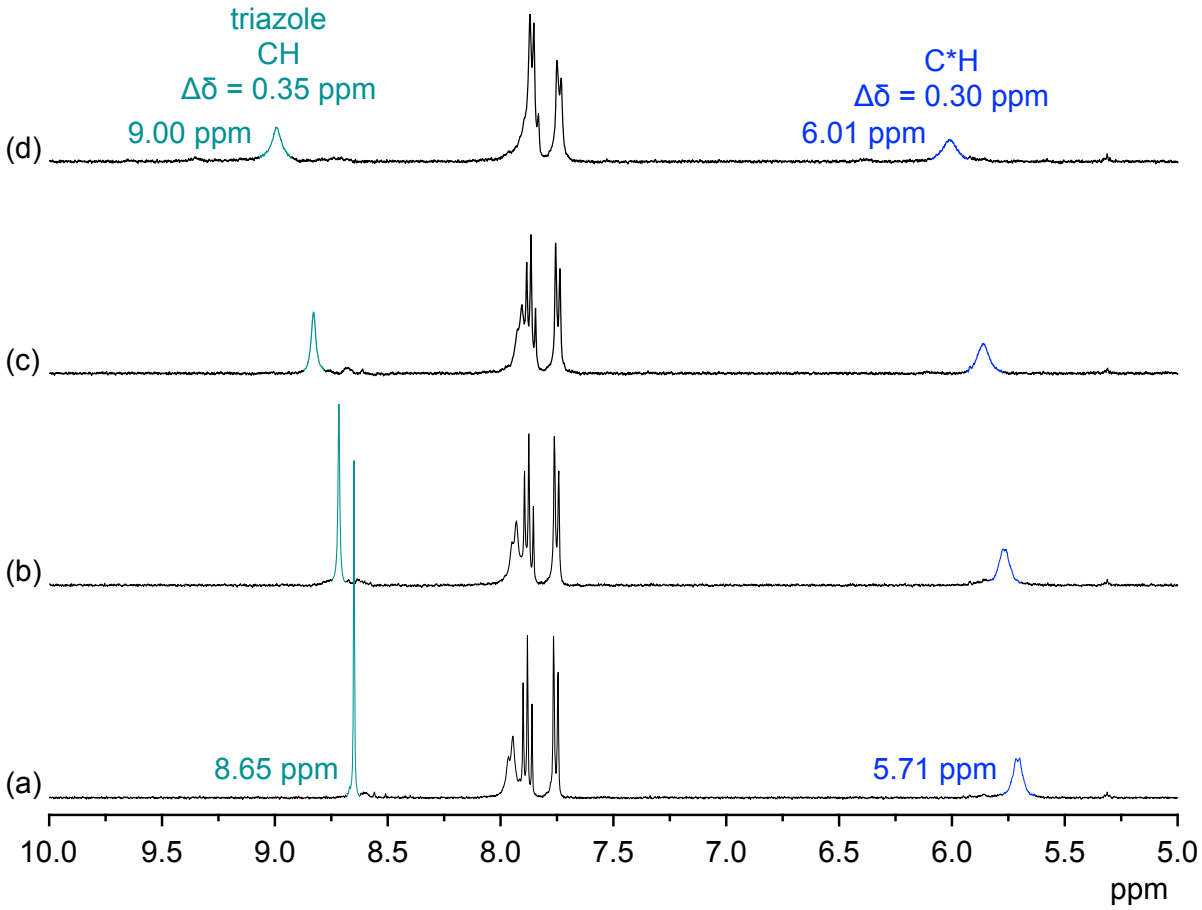

$^{1}$H NMR Spectra: **2** (0.5 mM) in 2.5 vol% $D_2O$/DMSO-$d_6$ in the absence (a) and the presence of 0.25 equiv (b), 0.5 equiv (c), 0.75 equiv (d), 1.0 equiv (e), and 2.0 equiv (f) of TBA HPP. The signals of the triazole and C*H protons are marked in green and blue, respectively.

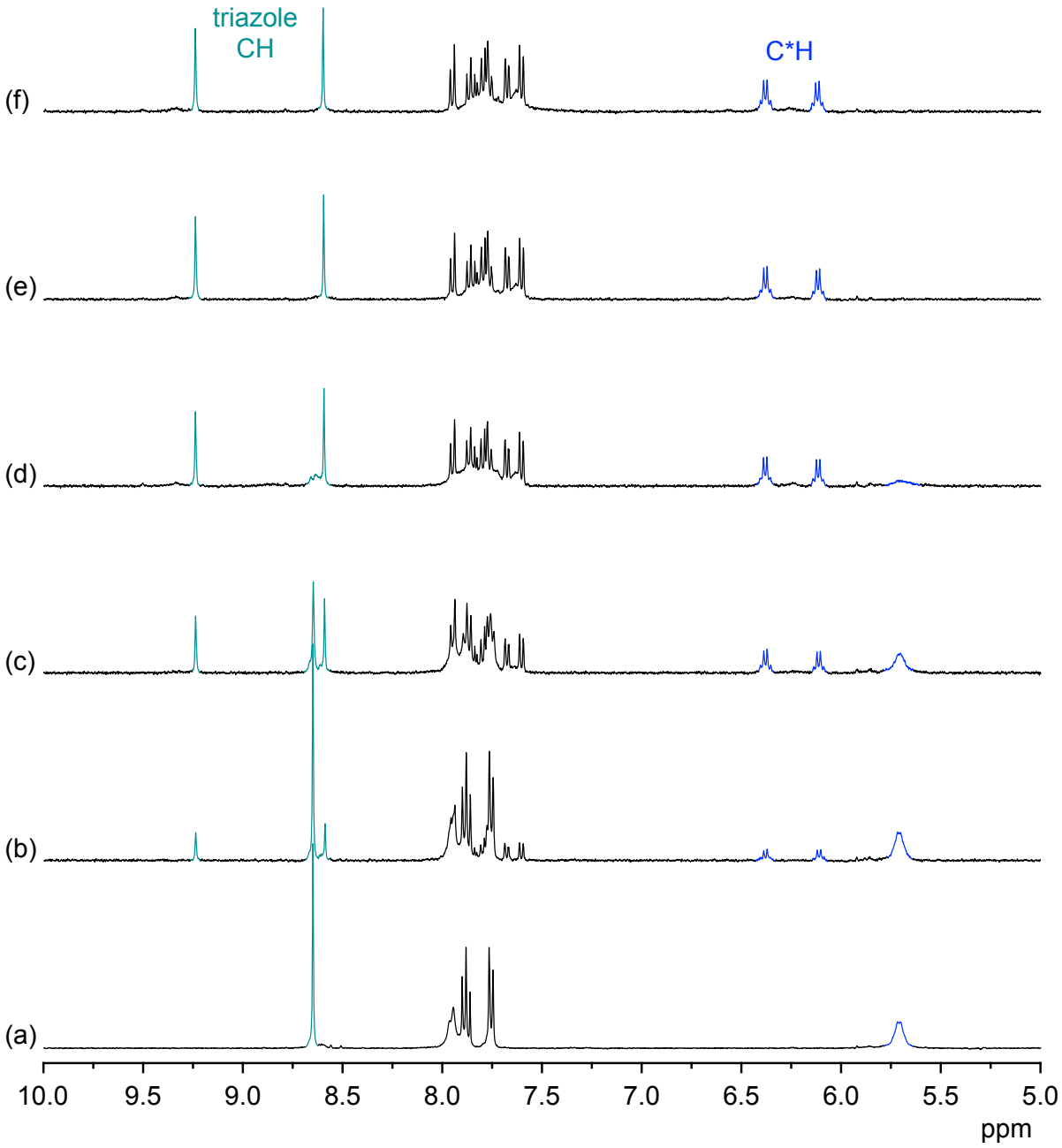

$^{1}$H NMR Spectra: TBA HPP (0.75 mM) in acetone-$d_6$ after 0 d (a), 3 d, (b), 5 d (c), 7 d (d), showing the formation of the aldol adduct of the solvent, deuterated 4-hydroxy-4-methylpentan-2-one. The signals assigned in red represent the residual protons of the mostly deuterated product.

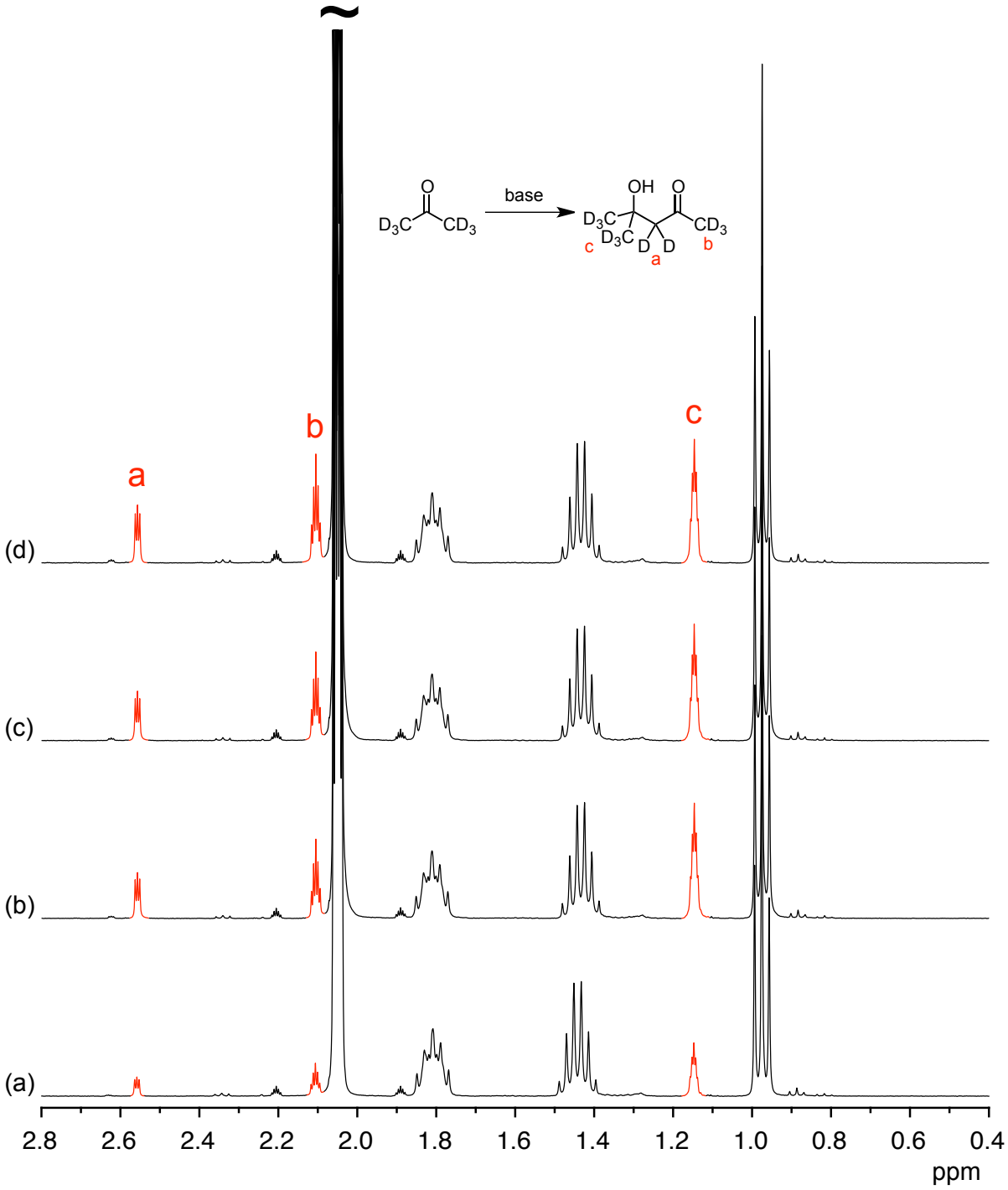

$^{1}$H NMR Spectra: **2** (0.5 mM) in acetone-$d_6$ in the presence of 1.5 equiv of TBA HPP after 0 d (a), 3 d, (b), 5 d (c), 7 d (d). The signals marked red again indicate the presence of the aldol adduct of the solvent, deuterated 4-hydroxy-4-methylpentan-2-one.

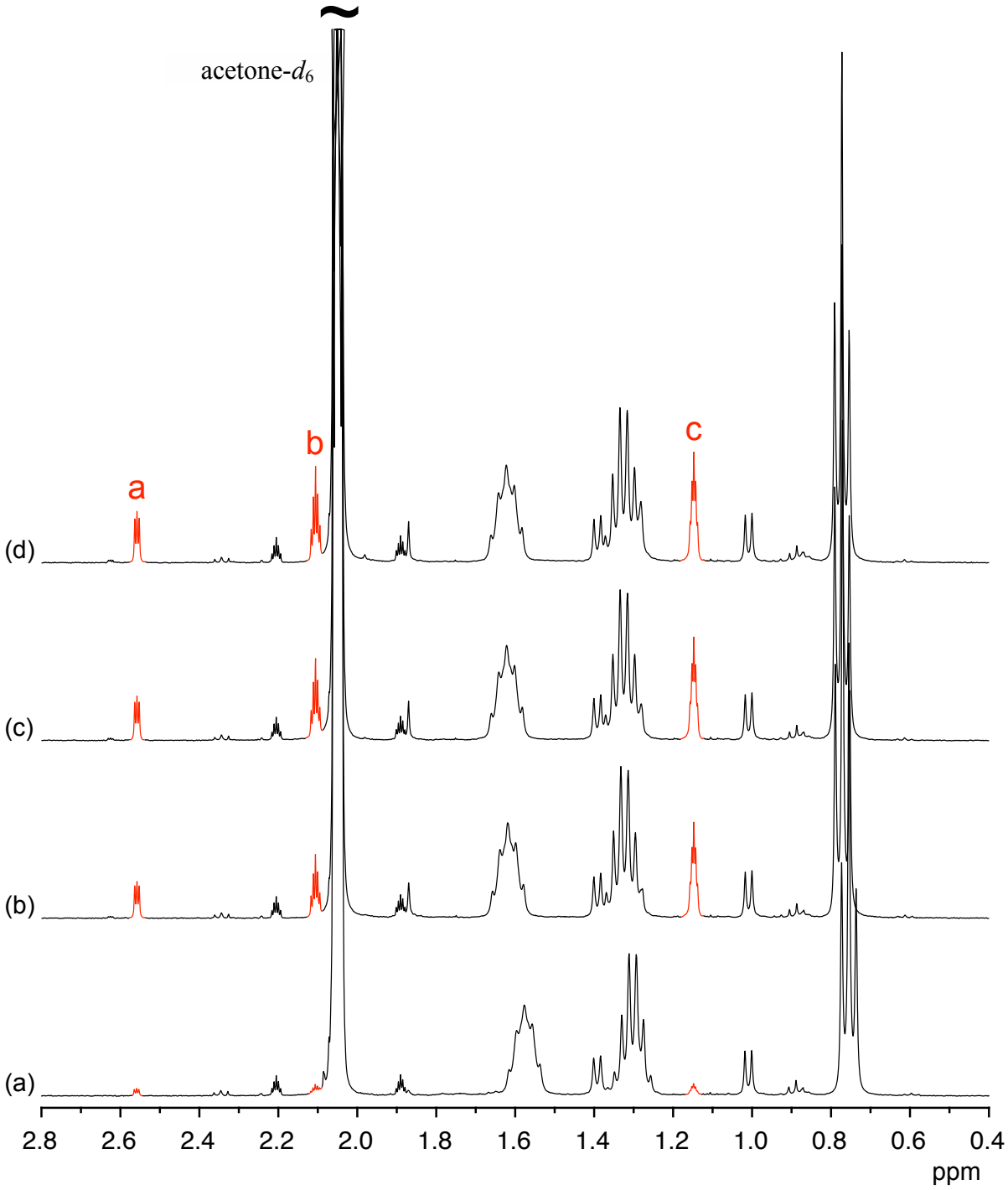

$^{1}$H NMR Spectra: **2** (0.5 mM) in acetone-$d_6$ in the presence of 1.5 equiv of TBA DHPP after 0 d (a), 3 d, (b), 5 d (c), 7 d (d). No signals of the aldol adduct are visible, indicating that the aldol adduct of acetone does not form in the presence of TBA DHPP.

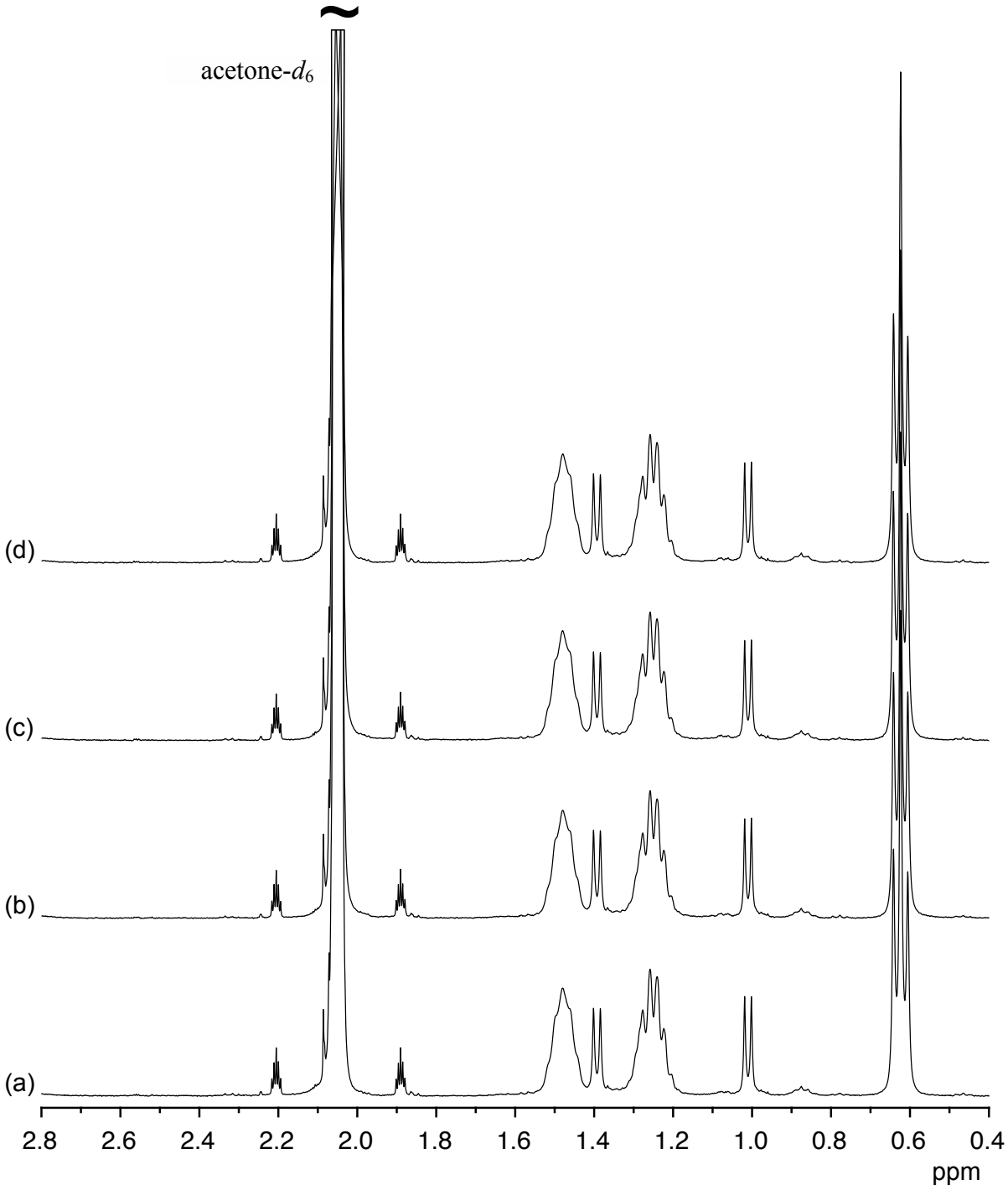

ESI MS: **2** (0.5 mM) in dichloromethane after the addition of TBA sulfate (1 equiv).

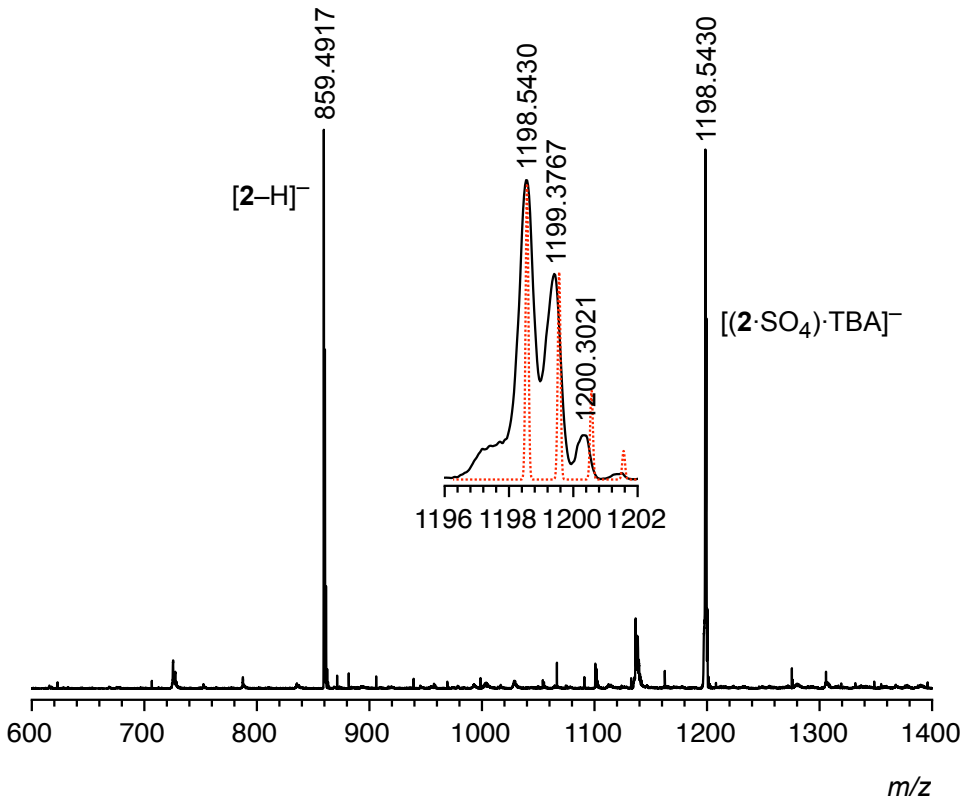


| | | *m/z calcd.* | *m/z exp.* |
|---|---|---|---|
| $[\mathbf{2}–H]^-$ | $C_{40}H_{36}N_{20}O_4 – H^+$ | 859.3558 | 859.4917 |
| $[(\mathbf{2}\cdot SO_4)\cdot TBA]^-$ | $C_{40}H_{36}N_{20}O_4 + SO_4^{2-} + C_{16}H_{36}N^+$ | 1198.5598 | 1198.5430 |

The dotted red line in the inset shows the calculated isotopic pattern of the respective peak.

ESI MS: **2** (0.5 mM) in dichloromethane after the addition of TBA DHPP (1 equiv).

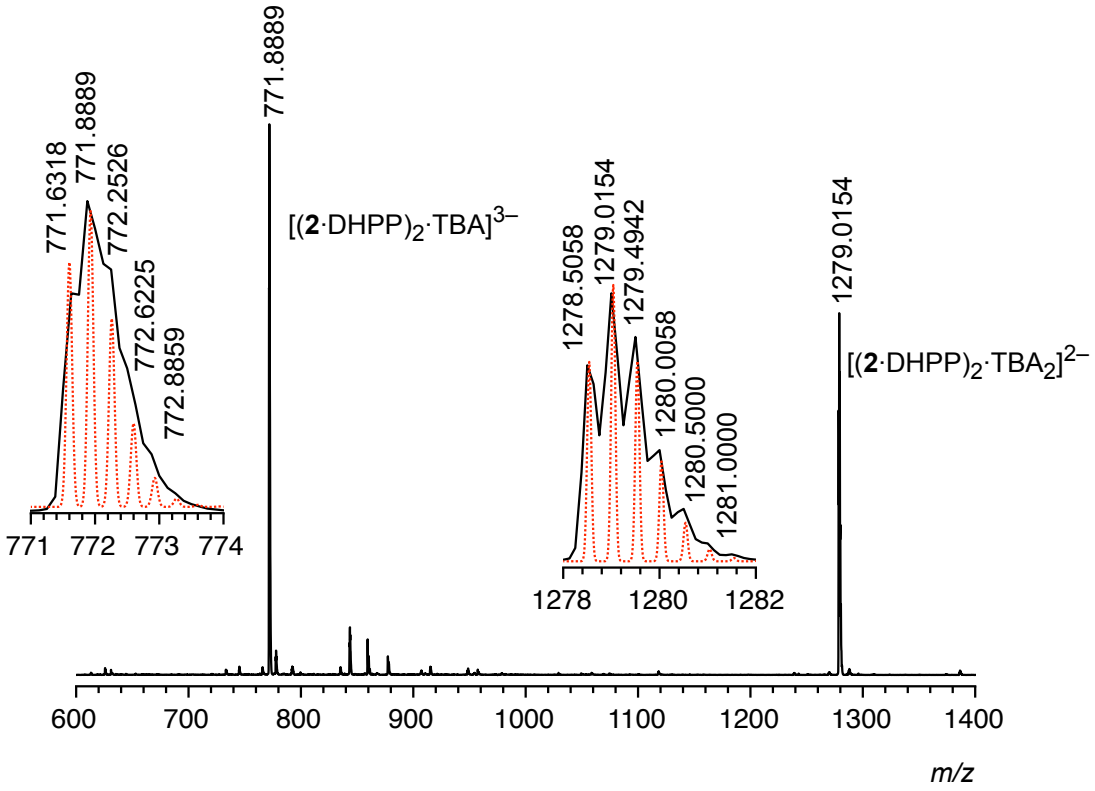


| | | *m/z calcd.* | *m/z exp.* |
|---|---|---|---|
| $[(\mathbf{2}\cdot DHPP)_2\cdot TBA]^{3-}$ | $(C_{40}H_{36}N_{20}O_4 + H_2O_7P_2)_2^{4-} + C_{16}H_{36}N^+$ | 771.9302 | 771.8889 |
| $[(\mathbf{2}\cdot DHPP)_2\cdot TBA_2]^{2-}$ | $(C_{40}H_{36}N_{20}O_4 + H_2O_7P_2)_2^{4-} + 2\ C_{16}H_{36}N^+$ | 1279.0374 | 1279.0154 |

The dotted red lines in the insets show the calculated isotopic pattern of the respective peak.

ESI MS: **2** (0.5 mM) in dichloromethane after the addition of TBA HPP (1 equiv).

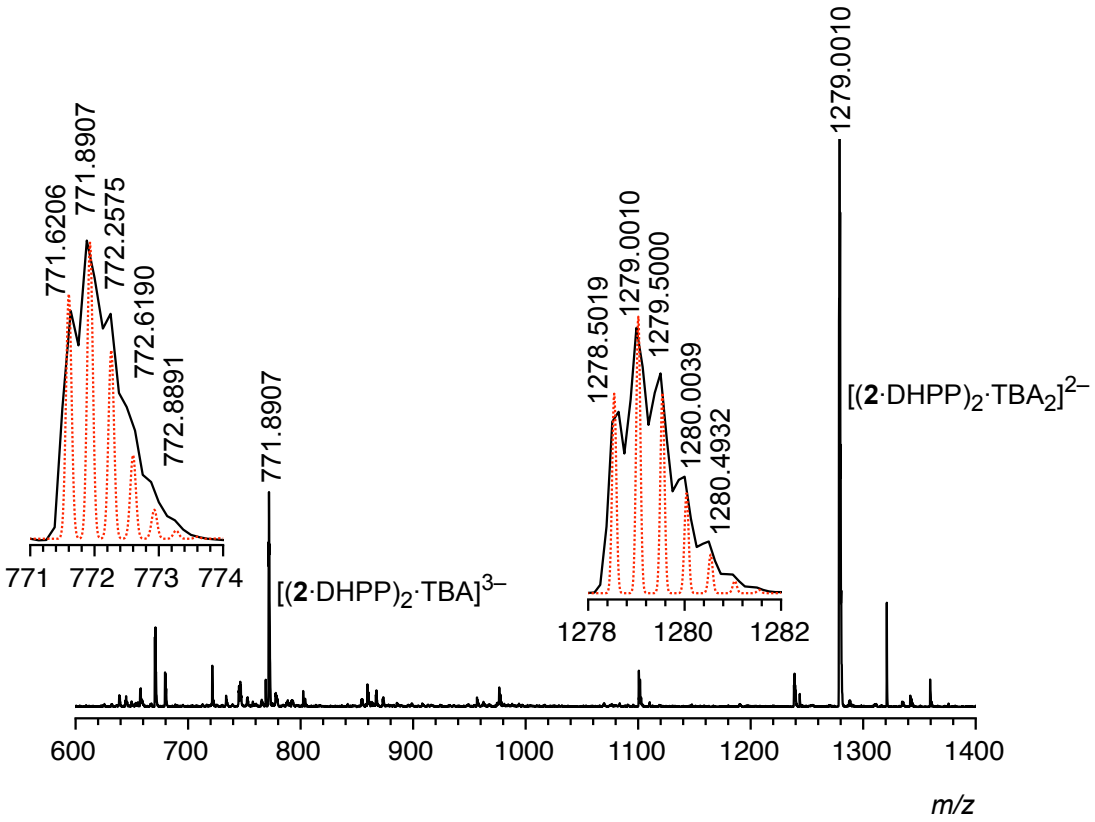


| | | *m/z calcd.* | *m/z exp.* |
|---|---|---|---|
| $[(\mathbf{2}\cdot\mathrm{DHPP})_2\cdot\mathrm{TBA}]^{3-}$ | $(C_{40}H_{36}N_{20}O_4 + H_2O_7P_2)_2^{4-} + C_{16}H_{36}N^+$ | 771.9302 | 771.8907 |
| $[(\mathbf{2}\cdot\mathrm{DHPP})_2\cdot\mathrm{TBA}_2]^{2-}$ | $(C_{40}H_{36}N_{20}O_4 + H_2O_7P_2)_2^{4-} + 2\ C_{16}H_{36}N^+$ | 1279.0374 | 1279.0010 |

The dotted red lines in the insets show the calculated isotopic pattern of the respective peak.

ESI MS: **2** (0.5 mM) in dichloromethane after the addition of TBA DHP (2 equiv).

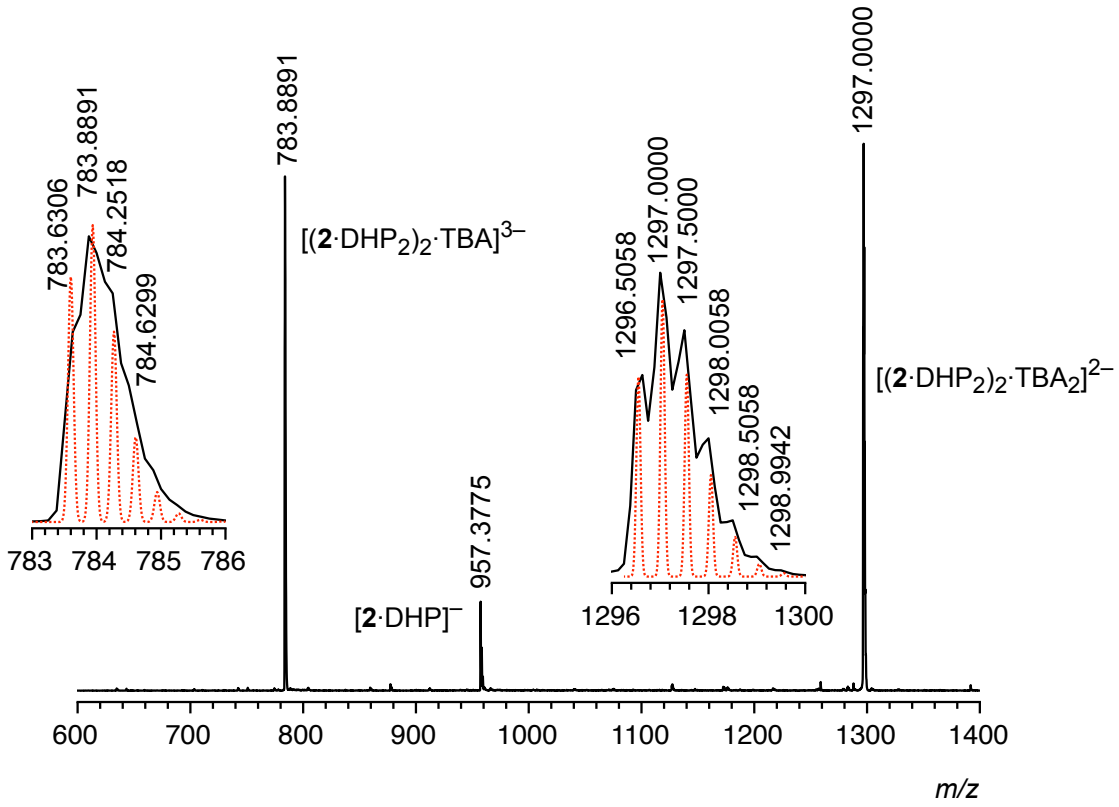


| | | *m/z calcd.* | *m/z exp.* |
|---|---|---|---|
| $[(\mathbf{2}\cdot DHP_2)_2\cdot TBA]^{3-}$ | $(C_{40}H_{36}N_{20}O_4 + (H_2O_4P)_2)_2^{4-} + C_{16}H_{36}N^+$ | 783.9372 | 783.8891 |
| $[\mathbf{2}\cdot DHP]^-$ | $C_{40}H_{36}N_{20}O_4 + H_2O_4P^-$ | 957.2924 | 957.3775 |
| $[(\mathbf{2}\cdot DHP_2)_2\cdot TBA_2]^{2-}$ | $(C_{40}H_{36}N_{20}O_4 + (H_2O_4P)_2)_2^{4-} + 2\ C_{16}H_{36}N^+$ | 1297.0480 | 1297.0000 |

The dotted red lines in the insets show the calculated isotopic pattern of the respective peak.

ITC Titrations:

The ITC experiments were carried out in 2.5 vol% water/DMSO. The anionic substrates were used as their TBA salts. The salts and receptor **2** were weighed using an analytical precision balance, dissolved in known volumes of the respective solvent mixture, and loaded into the system for immediate analysis.

The measurements were carried out at 25 °C using a reference power of 25 μJ/s, a filter period of 2 s, a stirrer speed of 307 rpm. Other experimental parameters of the individual titrations are specified in the Table S1. Automated baseline assignment and peak integration of raw thermograms were accomplished by singular value decomposition and peak-shape analysis using NITPIC.3[a] Estimation of best-fit parameter values by weighted nonlinear least-squares fitting and calculation of 68.3% confidence intervals were performed with the public-domain software SEDPHAT,3[b] as explained in detail elsewhere.3[c,d]

**Table S1**. Concentrations and experimental parameters of the individual titrations.

| guest anion as TBA salt | *c*(**2**) / mM | *c*(salt) / mM | injection volume / μL | no. of injections | spacing time / s |
|---|---|---|---|---|---|
| sulfate | 0.4 | 13.6 | 8 | 32 | 200 |
| DHPP | 0.4 | 6.1 | 8 | 32 | 200 |
| DHP | 0.4 | 12.9 | 8 | 34 | 200 |

Titration of **2** with TBA sulfate: The blue spheres show the experimental results and the red line the fitted curve calculated by using the one site binding model. The inset shows the heat pulses of the measurement from which the isotherm was generated.

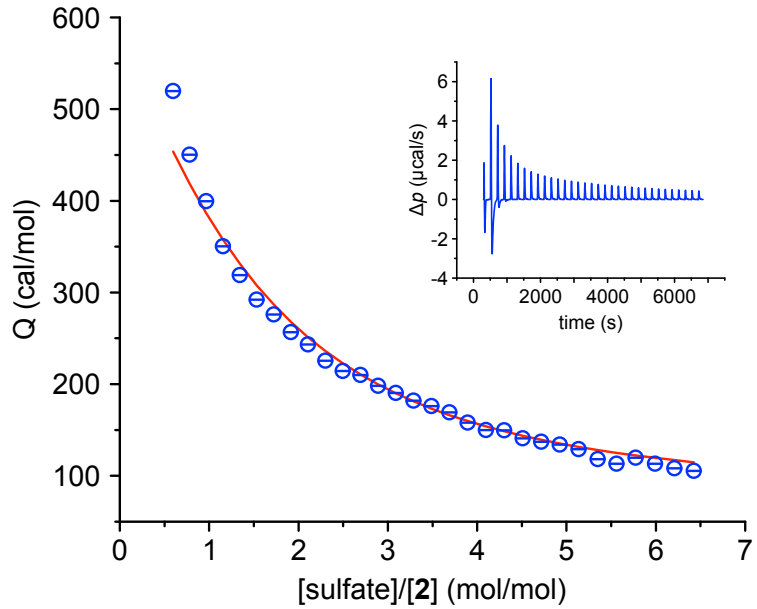


Titration of **2** with TBA DHPP: The blue spheres show the experimental results and the red line the fitted curve calculated by assuming that the dimer of the anion binds to two molecules of **2** in a stepwise fashion. The inset shows the heat pulses of the measurement from which the isotherm was generated.

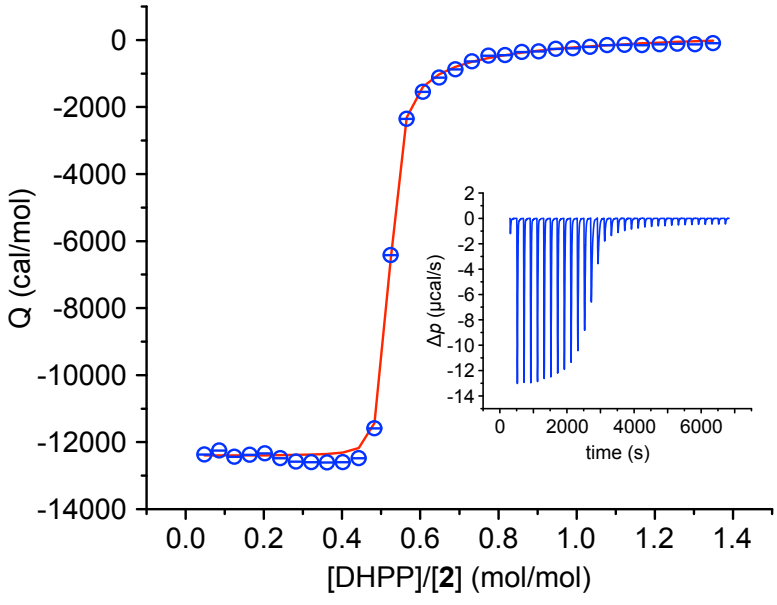

**Table S2**. Thermodynamic parameters for the binding of TBA DHPP to **2** under the assumption that the dimer of the anion $(DHPP)_2$ binds as a single entity to two molecules of **2** in a stepwise fashion.[a]

| reaction | log $K_a$ | $\Delta G$ | $\Delta H$ | $T\Delta S$ |
|---|---|---|---|---|
| **2** + $(DHPP)_2$ ⇌ [**2**·$(DHPP)_2$] | 6.3 | -36.2 | -33.2 | 3.0 |
| **2** + [**2**·$(DHPP)_2$] ⇌ [**2**·$(DHPP)_2$]$_2$ | 6.4 | -36.2 | -20.1 | 16.1 |
| 2 **2** + $(DHPP)_2$ ⇌ [**2**·$(DHPP)_2$]$_2$ | 12.7 | -72.2 | -53.3 | 19.1 |

[a] $\Delta G$, $\Delta H$, and $T\Delta S$ in kJ mol$^{-1}$.

Titration of **2** with TBA DHP: The blue spheres show the experimental results and the inset shows the heat pulses of the measurement from which the isotherm was generated.

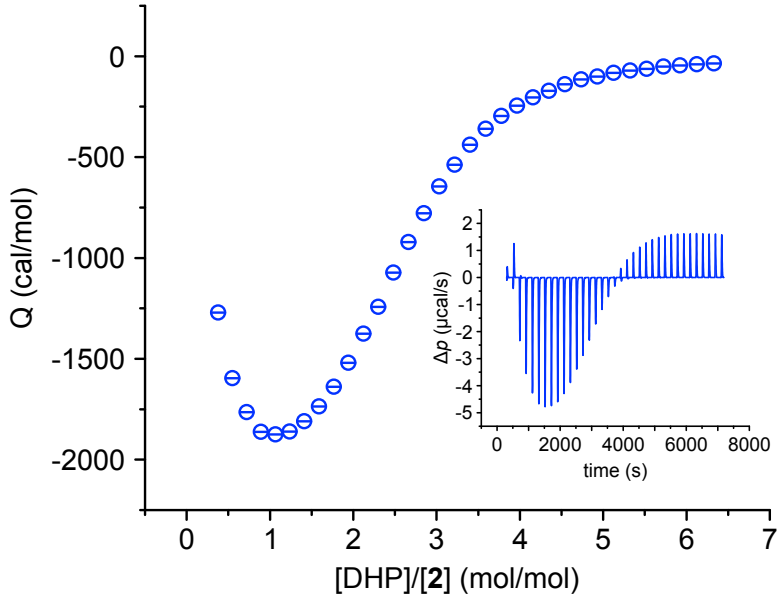

Crystal Structures:

**General details**. Single crystal X-ray data were collected at 120 K on an Agilent Super-Nova dual wavelength diffractometer with a micro-focus X-ray source and multilayer optics monochromatised CuKα (λ = 1.54184 Å) radiation. Program *CrysAlisPro*[4] was used for the data collection and reduction. The diffraction intensities were corrected for absorption using analytical face index absorption correction method[5] for all the data. The structures were solved with direct methods (*SHELXT*[6]) and refined by full-matrix least squares on $F^2$ using *SHELXL*-2016/6.[7] SQUEEZE module of PLATON[8] was utilised in the structure refinement to remove the residual electron densities, which were not possible to be reliably assigned and refined. Anisotropic displacement parameters were assigned to non-H atoms. Positional disorder in the structures was treated by restraining or constraining the geometric and anisotropic displacement parameters as gently as possible. All hydrogen atoms (except O-*H* in **$2_2$·DHPP$_2$** as well as O-*H* and N-*H* in **2(rac)$_2$·DHPP$_2$**) were refined using riding models with $U_{eq}$(H) of 1.5$U_{eq}$(C,O) for terminal methyl and hydroxyl groups, and 1.2 of $U_{eq}$(C,N) for other groups. The hydrogens found from the difference Fourier maps and bonded to O or N were refined with restrained ideal O-*H* (0.84 Å) or N-*H* (0.91 Å) distances and with $U_{eq}$(H) of 1.5 $U_{eq}$(O) or 1.2 $U_{eq}$(N). The additional details of each novel crystal data, data collection, and the refinement results are documented below (see also Table S3).

**Structure of $2_2$·DHPP$_2$**: $2_2$·DHPP$_2$ was crystallised as colourless prisms from a solution of **2** in DMSO containing 1 equiv of TBA DHPP. The structure found from the solution contains one (**$2_2$·DHPP$_2$**)$^{4-}$ and only two $TBA^+$ cations, while other molecular entities could not be located. The data is so badly disordered that according to analysis by PLATON/SQUEEZE[8] approximately 4500 electrons were removed in the procedure, which includes the ones of missing cations (and other unknown entities) and exceeds the $F$(000) value.

(a) (b)

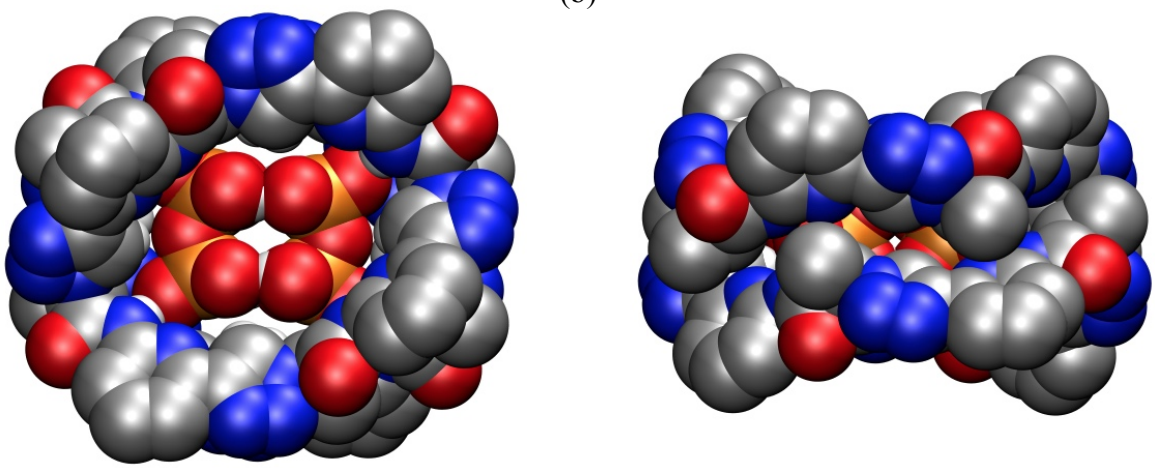

Figure S1: Molecular structure of **$2_2$·DHPP$_2$** as space-filling models showing the sandwich-type arrangement of the two pseudopeptide rings and the DHPP anion from the top (a) and the side (b). The TBA cations and the hydrogen atoms except those on the anion, NH and triazole CH groups are omitted for clarity.

**Structure of 2(rac)$_2$·DHPP$_2$**: **2(rac)$_2$·DHPP$_2$** with the exact composition $4(\mathbf{2}(\text{rac})_2\cdot\text{DHPP}_2)^{4-}\cdot 13(C_{16}H_{36}N^+)\cdot 9(C_6H_{12}O_2)\cdot(C_3H_6O)\cdot(H_2O)$ was crystallised as colourless plates from a solution of **2** in acetone containing 1 equiv of TBA HPP.

All the cations for the charge balance could not be located from the data. Almost 2000 electrons were removed in PLATON/SQUEEZE[8] procedure. The DHPP anions, as in **$2_2$·DHPP$_2$**, form pairs by hydrogen bonds with O···O distances between 2.49 and 2.55 Å. Similarly, the two pseudopeptides are holding the anion pair in the cavity between the rings with hydrogen bonds, which show N···O distances between 2.71 and 2.86 Å, as well as, C···O between 3.60 and 4.00 Å. The TBA cations outside the bowl-shaped cavity are filling the spaces between the complexes, which applies also for 4-hydroxy-4-methylpentan-2-one, acetone and water molecules. The nitrogen atoms in triazole molecules are accepting hydrogen bonds donated by 4-hydroxy-4-methylpentan-2-one and water molecules (O···N between 2.87 and 3.00 Å).

(a) (b)

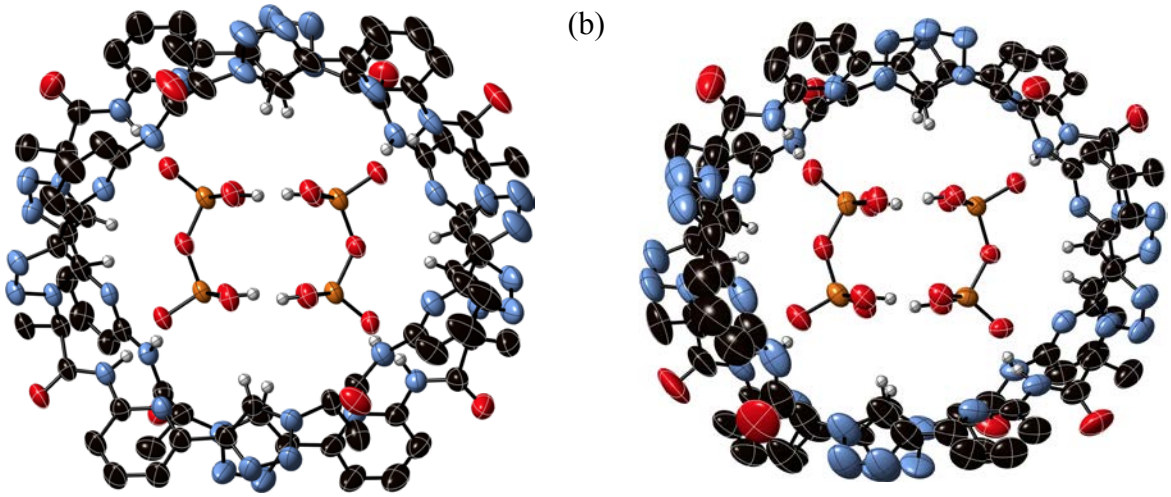

Figure S2: Molecular structure of **2(rac)$_2$·DHPP$_2$** showing the 2:2 association of the pseudopeptide and two DHPP anions with the thermal ellipsoids shown at the 50% probability level. Figure. S2a shows the complex of the all-*R* enantiomer of **2** and Figure S2b the one with the all-*S* enantiomer. TBA cations and the hydrogen atoms except those on the anion, NH and triazole CH groups are omitted for clarity.

Another batch of **2(rac)$_2$·DHPP$_2$** crystals was obtained from DMSO/DCM, 1:1 (*v*/*v*). The structure solution of these crystals has the composition $3(\mathbf{2(rac)}_2\cdot DHPP_2)^{4-}\cdot 12(C_{16}H_{36}N)^{+}\cdot 8(C_2H_6OS)\cdot 3.2H_2O$ (H atoms for water molecules were not found). In this **2(rac)$_2$·DHPP$_2$-2** structure only 200 electrons were removed by PLATON/SQUEEZE.[8] Hydrogen bonding O···O distances in DHPP dimer shows values between 2.51 and 2.67 Å. Hydrogen bonds between pseudopeptides and anions show N···O distances between 2.67 and 2.98 Å, and C···O distances between 2.98 and 3.80 Å. Five of the six bowl-shaped cavities of pseudopeptide rings are filled by TBA cations, while one cavity is occupied by DMSO molecules. The remaining TBA cations are located between the complexes.

(a) (b)

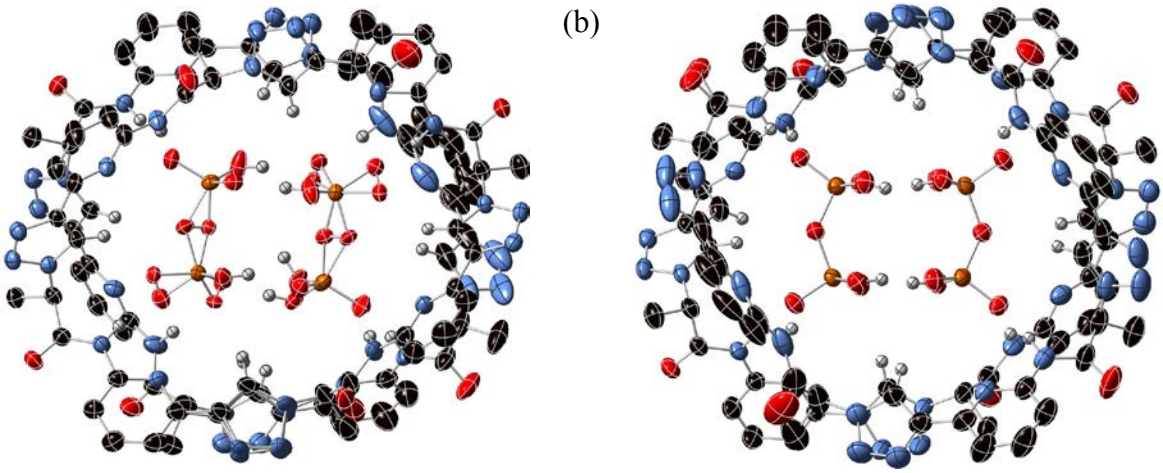

Figure S3: Molecular structure of **2(rac)$_2$·DHPP$_2$-2** showing the 2:2 association of the pseudopeptide and two DHPP anions with the thermal ellipsoids shown at the 50% probability level. Figure. S3a shows the complex of the all-*R* enantiomer of **2** and Figure S3b the one with the all-*S* enantiomer. TBA cations and the hydrogen atoms except those on the anion, NH and triazole CH groups are omitted for clarity.

**Structure of $2_2$·DHP$_4$**: **$2_2$·DHP$_4$** with the exact composition $4(\mathbf{2}_2 \cdot DHP_4)^{4-} \cdot 11(C_{16}H_{36}N)^{+} \cdot (C_2H_6OS)$ was crystallised as colourless plates from a solution of **2** in DMSO, containing 2 equiv of TBA DHP. Note that also in this structure not all of the TBA cations could be located because of substantial disorder. in addition, part of the structure containing almost 3500 electrons was removed by PLATON/SQUEEZE.[8]

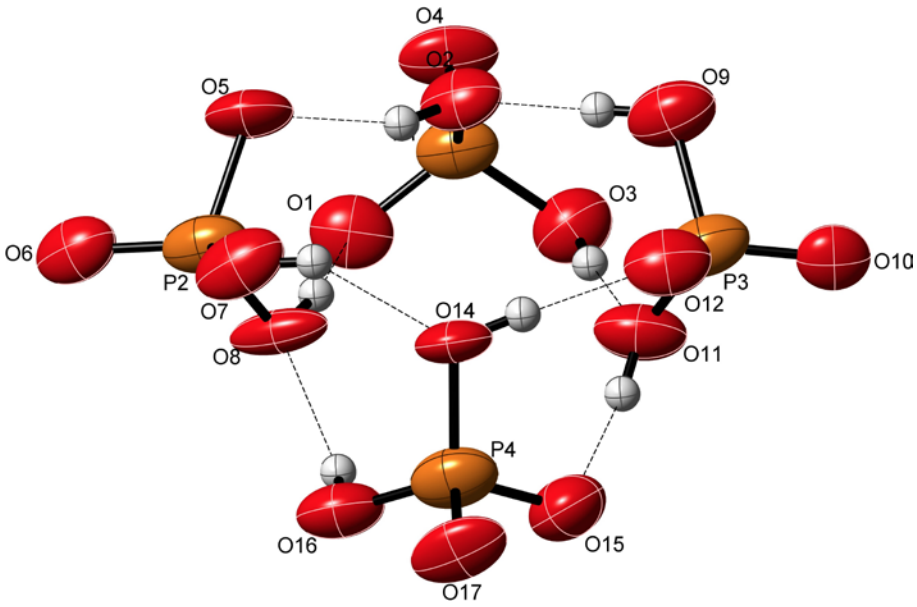


Figure S4: Detailed representation of the hydrogen bonding pattern in the DHP tetramer of $\mathbf{2_2 \cdot DHP_4}$.

(a) (b)

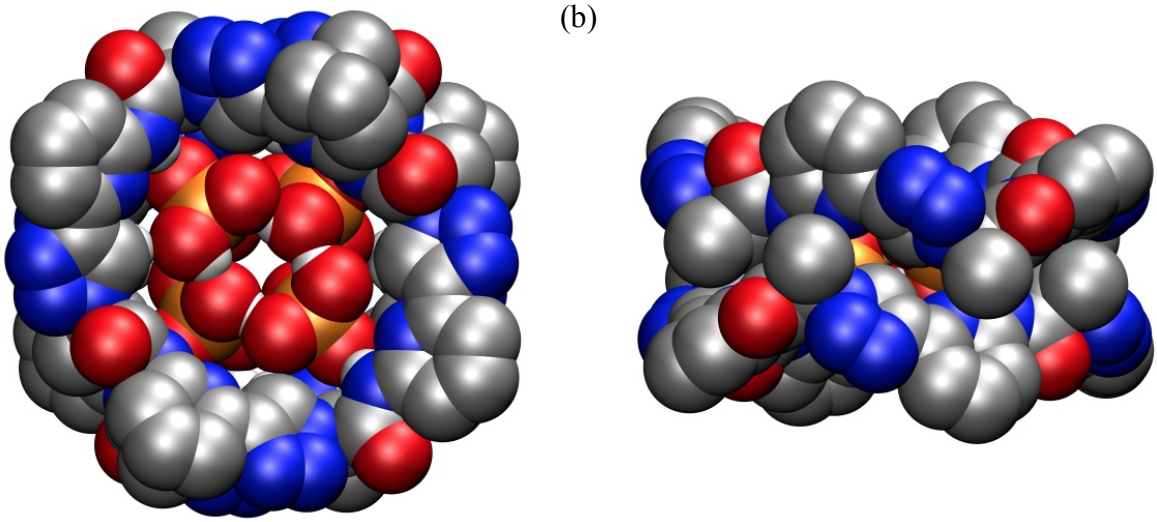

Figure S5: Molecular structure of $\mathbf{2_2 \cdot DHP_4}$ as space-filling models showing the sandwich-type arrangement of the two pseudopeptide rings and the DHPP anion from the top (a) and the side (b). The TBA cations and the hydrogen atoms except those on the anion, NH and triazole CH groups are omitted for clarity.

**Table S3**. Crystal data and parameters for **$2_2$·DHPP$_2$**, **2(rac)$_2$·DHPP$_2$**, **2(rac)$_2$·DHPP$_2$-2**, and **$2_2$·DHP$_4$**.

| | **$2_2$**·DHPP$_2$ | **2**(rac)$_2$·DHPP$_2$ | **2**(rac)$_2$·DHPP$_2$-2 | **$2_2$**·DHP$_4$ |
|---|---|---|---|---|
| CCDC number | 1555955 | 1555956 | 1555957 | 1555958 |
| Empirical formula | $C_{56}H_{74}N_{21}O_{11}P_2$ | $C_{585}H_{888}N_{173}O_{108}P_{16}$ | $C_{224}H_{354}N_{66}O_{38.61}P_6S_4$ | $C_{498}H_{722}N_{171}O_{97}P_{16}S$ |
| $F_W$ [g/mol] | 1279.30 | 12568.15 | 4903.61 | 11184.00 |
| Crystal system | Trigonal | Triclinic | Triclinic | Monoclinic |
| Space group | $P321$[a] | $P$-1 | $P$-1 | $P2_1$[b] |
| Unit cell dimensions | | | | |
| $a$ [Å] | 28.3369(4) | 22.1903(3) | 28.2322(3) | 26.9085(8) |
| $b$ [Å] | 28.3369(4) | 31.9713(4) | 28.4659(3) | 36.1230(11) |
| $c$ [Å] | 58.9056(13) | 61.8821(4) | 39.1611(5) | 41.160(3) |
| $\alpha$ [°] | 90 | 76.0283(8) | 72.4310(10) | 90 |
| $\beta$ [°] | 90 | 79.8139(8) | 82.4440(10) | 92.306(4) |
| $\gamma$ [°] | 120 | 73.4101(11) | 60.3890(10) | 90 |
| $V$ [Å$^3$] | 40963.0(15) | 40554.3(8) | 26079.5(6) | 39975(3) |
| $Z$ | 6 | 2 | 4 | 2 |
| $\rho$ [Mg/m$^3$] | 0.311 | 1.029 | 1.249 | 0.929 |
| $\mu$ [mm$^{-1}$] | 0.290 | 0.878 | 1.330 | 0.857 |
| $F$(000) | 4050 | 13426 | 10492 | 11878 |
| Crystal size [mm] | 0.25×0.25×0.07 | 0.30×0.21×0.08 | 0.40×0.27×0.09 | 0.18×0.15×0.04 |
| $\theta$ range [°] | 3.462 − 67.994 | 3.511 − 69.999 | 3.365 − 67.999 | 3.448 − 67.700 |
| Reflections collected | 121482 | 238782 | 453951 | 237482 |
| Independent reflections | 49626 | 147346 | 94326 | 141768 |
| $R_{int}$ | 0.0697 | 0.0446 | 0.0656 | 0.2577 |
| Reflections [$I>2\sigma(I)$] | 35387 | 91821 | 72636 | |
| Restraints / parameters | 561 / 789 | 1968 / 8199 | 2100 / 6486 | 3051 / 6845 |
| Completeness to $\theta$ [%] | 99.9 | 97.5 | 99.4 | 99.8 |
| Max.&min transmission | 0.951 & 0.879 | 0.925 & 0.806 | 0.921 & 0.762 | 0.949 & 0.844 |
| Goodness-of-fit on $F^2$ | 1.355 | 1.025 | 1.671 | 0.941 |
| Final $R$ [$I>2\sigma(I)$] | R1 = 0.1378 | R1 = 0.0800 | R1 = 0.1161 | R1 = 0.1303 |
| | wR2 = 0.3698 | wR2 = 0.2302 | wR2 = 0.3604 | wR2 = 0.3123 |
| $R$ (all data) | R1 = 0.1571 | R1 = 0.1171 | R1 = 0.1375 | R1 = 0.2948 |
| | wR2 = 0.3929 | wR2 = 0.2710 | wR2 = 0.3926 | wR2 = 0.4534 |
| Largest peak&hole [e./Å$^3$] | 0.563 & -0.544 | 0.873 & -0.678 | 1.967 & -2.065 | 0.578 & -0.591 |

Absolute structure parameter: [a] meaningless and removed; [b] 0.11(4)

References


1 H. E. Gottlieb, V. Kotlyar and A. Nudelman, *J. Org. Chem.*, 1997, **62**, 7512-7515.

2 D. Mungalpara, H. Kelm, A. Valkonen, K. Rissanen, S. Keller, S. Kubik *Org. Biomol. Chem.*, 2017, **15**, 102-113.

3 (a) S. Keller, C. Vargas, H. Zhao, G. Piszczek, C. A. Brautigam and P. Schuck, *Anal. Chem.*, 2012, **84**, 5066-5073; (b) J. C. D. Houtman, P. H. Brown, B. Bowden, H. Yamaguchi, E. Appella, L. E. Samelson and P. Schuck, *Protein Sci.*, 2007, **16**, 30-42; (c) G. Krainer, J. Broecker, C. Vargas, J. Fanghänel and S. Keller, *Anal. Chem.*, 2012, **84**, 10715-10722; (d) G. Krainer, S. Keller, *Methods*, 2015, **76**, 116-123.

4 *CrysalisPro* 2015, Rigaku OD, version 1.171.38.41.

5 R. C. Clark and J. S. Reid, *Acta Crystallogr., Sect. A: Found. Crystallogr.*, 1995, **51**, 887.

6 G. M. Sheldrick, *Acta Crystallogr., Sect. A: Found. Adv.*, 2015, **71**, 3-8.

7 G. M. Sheldrick, *Acta Crystallogr., Sect. C: Struct. Chem.*, 2015, **71**, 3-8.

8 (a) Spek, A. L. *Acta Crystallogr., Sect. C: Struct. Chem.*, 2015, **71**, 9-18. (b) A. L. Spek, *Acta Crystallogr., Sect. D: Biol. Crystallogr.*, 2009, **65**, 148-155.